DESIGN OF A FATIGUE TESTING MACHINE WITH AXIAL DISPLACEMENT FOR COMPOSITE MATERIALS.

FINAL PROJECT ERASMUS

Politechnika Wrocławska
Wydział Mechaniczny

Written by:

Pablo López Carpena.

Supervised by:

Dr. Grzegorz Lesiuk and Manuel Tur Valiente.

INDEX.

1. INTRODUCTION.

This is a project carried out for the Wroclaw University of Science and Technology for the Erasmus project, made by Pablo López Carpena (268982) and supervised by Dr. Grzegorz Lesiuk and Manuel Tur Valiente.

2. OBJECTIVE OF THE PROJECT.

The objective of the project is to modify an existing fatigue testing for carrying out a fatigue test on composite rebars testing, with the actual fatigue machine is impossible to carry out this experiment due the premature breakage of the specimens. The specimens are basically GFRP (Glass Fibber Reinforced Polymer), BFRP (Basalt Fibber Reinforced Polymer) and a combination of both, later will be more information about the specimens. The main goal is to adapt the movement of the actual machine into an axial movement.

3. FACTORS TO BE CONSIDERED.

3.1 Conditions of the design.

The conditions that have been considered during the design process are the following ones:

- The system is designed to make test of materials with breaking limits between:

  Su=200-1500 MPa.

- The number of cycles.

  This machine is designed as a Low Cycle Fatigue machine cause of the properties of the composite rebars.

- Possibility to test specimens with different diameters.

    D=6~10 mm.

- Possibility to make different test changing the configuration of the machine. In this case, four different configurations in order to have a deformation on the samples of five, ten, fifteen and twenty millimetres, depending on the configuration selected.

- The dimensions of the system are conditioned by the limits where the system has to be constructed, always seeking the maximum efficiency in the use of space.

3.2 Current legislation.

Here are presented the main standards used in the design:

- Designation: D7205/D7205M for Standard test method for tensile properties of fiber reinforced matrix composite bars.

4. ANALYSIS OF THE FATIGUE TESTING MAHINES

Fatigue can be characterized as the phenomenon of progressive failure consisting of the initiation and propagation of cracks, which can reach a sufficient size to cause fracture. This occurs in ductile materials below the yield strength, and in fragile materials below the tensile break limit. This phenomenon appears after the material is subjected to cyclic loads for a certain period of time or a certain number of cycles. The final failure produced by the crack generally is fast, and very difficult to notice cause doesn't exist a previous big deformation. The lack of deformation before the failure makes it very difficult to detect by mere visual inspection, causing breaks without previous warnings. However, the fatigue process starts with the beginning of the

component's use, and it's used to be located in specific areas of the component where stresss and deformations are concentrated due to external charges, changes in geometry, imperfections of the material, differences of temperature, …

4.1 Phases of the fatigue process.

- Nucleation, this is the first stage of the process where the crack is started, this crack is generated near to the material defects and in stress concentrators such as notches, holes for screws and so on. This is propagated along the crystallographic planes with greater shear stress. The surface crystals are less supported than the interiors, so in them it is easier to slide. The Ambiental's conditions can also influence in the creation of this process.

- Propagation of the crack, the crack grows rapidly with each charge cycle. The direction of propagation is also different and is more favored in directions perpendicular to the applied stress.

- Final breakage, when the crack has reached the critical size, spreads very quickly along the piece producing the rupture.
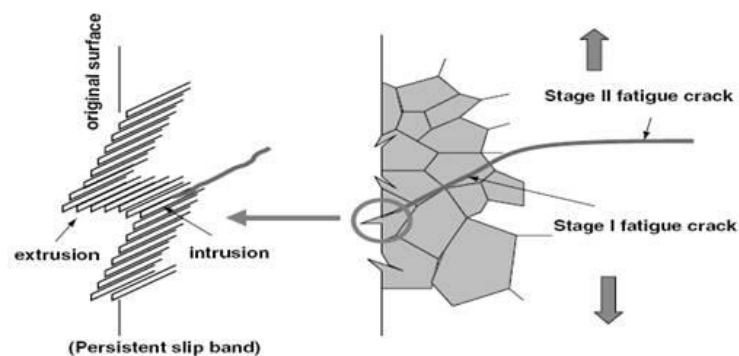

Image1. Stages of fatigue process.

These three processes appear always on the fatigue life of a piece. The velocity of this process depends on the stress applied to the material, is also necessary to know that the third stage is not taken into account for the determination of the life of a material, cause this process is instantaneous. In the application of small stresss, the phase of creation of the crack covers the biggest in the life of the piece. For bigger stresss, the phase of propagation is a fundamental factor to determinate the life of a piece. To define the cycles supported by the material, there are three parameters Nf (the total number of cycles supported), Ni (number of cycles during the nucleation) and Np (number of cycles during the propagation).

$$Nf = Ni + Np$$

4.2 High Cycle Fatigue and Low Cycle Fatigue.

The fatigue test can be easily divided into two groups depending on the number of cycles applied to the piece before the breakage.

- During the High Cycle Fatigue test is required at least 10^4 cycles to cause the failure, the stress is low and primarily elastic, so the plastic deformation never occurs during this process. In this case, stresss and deformations are considered proportional and it's possible to use a stress analysis.

- The Low Cycle Fatigue is characterized by repeated plastic deformation, applied in every cycle so the number of cycles is lower. The stresss applicated are higher, due to this It's impossible to create a relation between stresss and deformations. Sometimes the life of the product it's not defined when the breakage is reached. When the crack reaches a determined size, can also be the end of the life of the product.

4.3 Wöhler Curves (S-N).

Like other properties we can also determine the fatigue resistance of the different materials by determining the S-N curve. The curves are draw by performing tests with cyclic loads that vary in amplitude, these cyclic loads will be explained after. Normally, tests are started with big amplitude values, S. On the order of two-thirds of the elastic limit of the material. When the specimen breaks, the number of cycles performed until the rupture are annotated. Then, the process is now repeated with another specimen and with lower amplitude values by annotating the life cycles again before the failure.
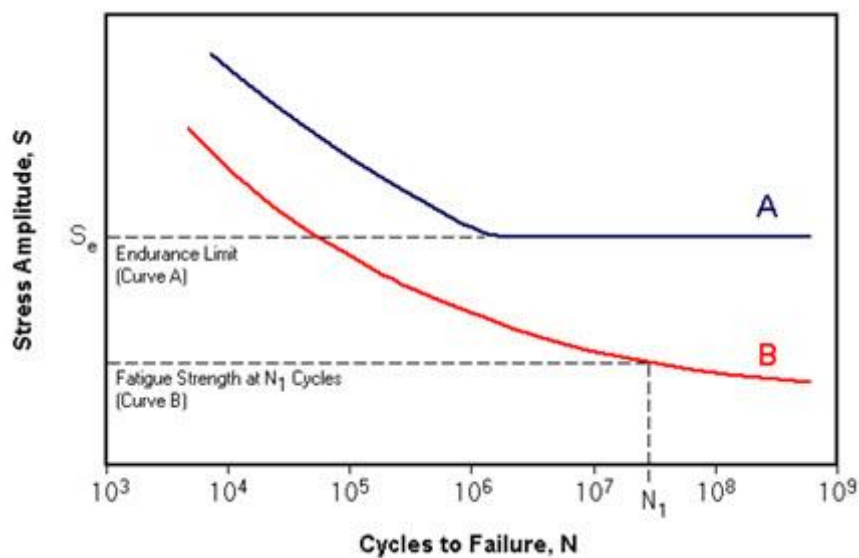

Image2. S-N curve example.

Analysis of the *Image2.*

- Curve A, in this case we can see the material have reached a point called the endurance limit, at this value of stress the breakage of the material won't happen. Under this line we can say that the material has an endless life, this is not correct and can be demonstrated by test with a really high number of cycles, but this is a field in process of study.

- Curve B, there are materials with elements such as aluminium, copper or magnesium that don't have Endurance Limit. This is reflected in the S-N curves that continues to decrease when we increase the number of cycles. For this type of materials, the parameter that will define its behaviour will be the resistance to fatigue, defined as the amplitude of stress that will produce the rupture for a certain number of cycles.

4.4 Composite rebars.

In this project the main goal is to perform the fatigue test for composite rebars and there are points that is necessary to consider in the application of cyclic loads and Wöhler curves. Composite rebars are materials that are laminate. A laminate is a highly heterogeneous material that presents a great anisotropy. These two properties influence their behavior and how the mechanism of degradation due to fatigue is presented. Heterogeneity is the main factor that marks the response of these materials subjected to cyclic loads. This contributes to the complexity of stress states associated with the development of fatigue damage, even before starting the process of degradation. The existence of different phases with different properties is the trigger of the local degradation mechanisms that act by initiating the process of damage. On the other hand, it is a factor that contributes laminated composite materials presenting a good resistance to fatigue. The expansion of damage is slowed by the presence of discontinuities between adjacent plates, or between different phases, due to their difference in properties and behavior.

4.4.1   S-N curves.

The rupture of a composite material reinforced with long fibers caused by cyclic loads is a progressive process in which different mechanisms of degradation of the laminate appear and combine. The appearance of small cracks in the matrix can become in a propagation of these cracks until there is a breakage of fibers in the adjacent areas and a local delamination between the sheets. The mechanism that produces fatigue is not based in nucleation and propagation, as

8

the case of metals. Anyway, many of the works with composite fatigue testing use the knowledge previously used in metals. This equivalence in the treatment of the fatigue phenomenon lies in assuming that the mechanisms that originate the fatigue behavior of the material are the same for metals and for composite.

4.4.2   Cyclic charges.

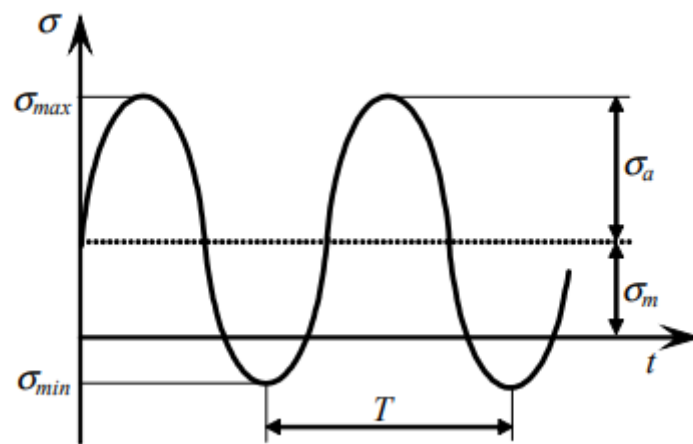The fatigue behavior of any material depends not only on the maximum level of stress to which it is subjected but also on the type of cyclic stress it receives.

Image3. Cyclic charge and his parameters.

The most important parameters are:

- The maximum and minimum stress values (σmax and σmin).

- The reversion ratio.

$$R = \frac{\sigma min}{\sigma max}$$

- The medium stress.

$$\sigma m = \frac{\sigma max}{2} + \frac{\sigma min}{2}$$

- Alternate stress.

$$\sigma a = \frac{\sigma max}{2} - \frac{\sigma min}{2}$$

- Other parameter as the frequency, have a very small impact.

With the reversion ratio it's possible to identify the type of stress applied.

- Values between -∞ and 0 indicate a tensile-compression stress (T–C).

- Values between 0 and +1 indicates tensile-only stress (T–T).

- Values between +∞ and +1 define compression-only stresses (C–C).

4.5 Analysis of existing fatigue machines.

In order to analyse the different types of fatigue machines with different types of applications, the machines will be divided into different sections.

4.5.1 Rotating bending testing machine.

These machines consist of an electric motor that rotates at a constant number of revolutions per minute while a stationary and constant load is applied on the specimen, so that it appears as a result, a constant bending moment on the specimen.

They are machines used for the testing of circular specimens and round bars according to DIN 50113.
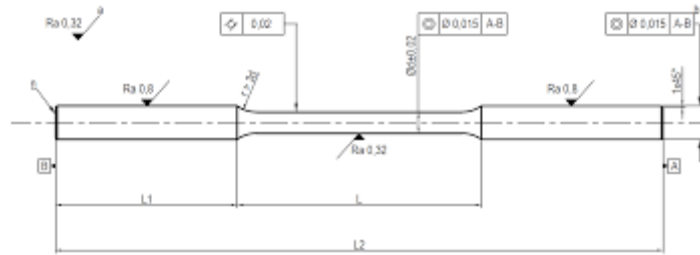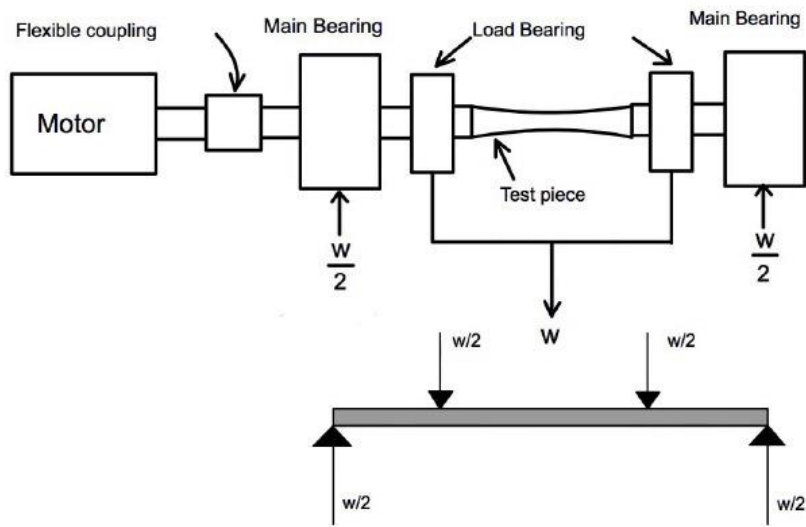
Image4. Specimen with the standards of DIN50113.

Image5. Scheme of a rotating bending fatigue machine.

This bending moment applied to a specimen that is rotating, causes the stresses at any point on the surface of the specimen to go from zero to the maximum traction, back to zero and then to the minimum compression, completely reversing the stressal state of a point throughout a cycle.
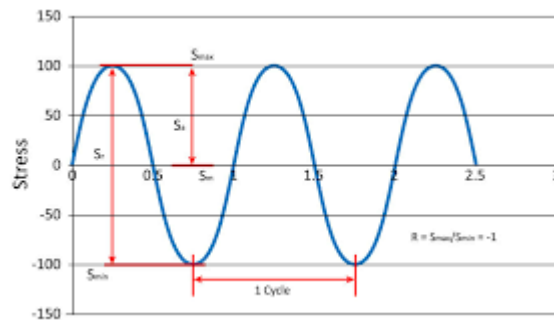

Image6. Cycle load in rotating bending fatigue machine.

The disadvantages of this type of machine are the impossibility of testing specimens with rectangular sections and the rigidity in the supports. The use of fixed prevent longitudinal displacements of the specimen and have associated reactions that are transmitted to the specimen. As result polymeric or polymer matrix materials such as carbon fiber should not be studied within this theory since the stresses that appear substantially affect the test.

4.5.2 Universal traction machine. Axial load fatigue tests.

These are machines for testing with tensile-compression loads. The machine works by applying dynamic axial loads of tensile-compression to the specimen. Universal machines are usually used to carry out this test that allow both static and dynamic tests.

The advantage of these machines, in addition to their versatility, is the study of specimens and parts of different characteristics. Rectangular, circular specimens, complex geometries, pieces with and without notches can be tested.

Image7. Axial load fatigue machines.   *Image8. Axial load fatigue machines.*

The *image7*, is one of the machines used for the inspiration of this project.

4.5.3   Resonance fatigue machine.

This analysis is possible by using machines with piezoelectric transducers that transform the electrical signal into a mechanic of the same frequency. It is possible in this way to test with frequencies close to 20KHz, or higher. Their low energy consumption and virtually maintenance-free drive make them an efficient alternative to servo hydraulic machines. In ultrasonic fatigue tests the machine and the specimen form a resonant system, so the specimen must be designed so that the first vibration mode matches the frequency of operation of the machine, the machine operates in a narrow range of frequencies, and it is not possible to use it to study the behavior of materials at a low number of cycles. These machines require costly maintenance and have a high price.

5.   IDEA OF CONTROL DISPLACEMENT MACHINE.

5.1 Concept.

The concept of a control displacement machine refers to the process of applying a load to a composite part of a machine. There are two principal process the load control and the displacement control, the last one is the concept applied to this machine and the explanation is the following one. In a displacement control machine the loads are

5.2 Design.

First of all, the main purpose is to design a machine prepared to carry out axial loads fatigue test. To do this with the actual machine the most important thing is to transform the rotating movement into an axial displacement. To do this, a pulley will be used to transfer the rotating movement of the actual machine to a disc connected with the new machine.
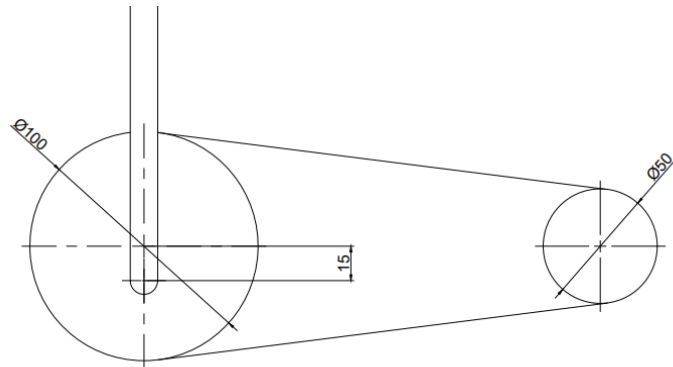
Image9. Pulley and belt connexion, on the left the rotating disc and on the right the motor.

The rotating disc connected to the machine have a bar connected 15 mm away from the centre, this means in every cycle of the machine the diameter of the movement of the beam is 30mm. This movement is transferred to the machine, causing a displacement in the point of the connexion of 30 mm.
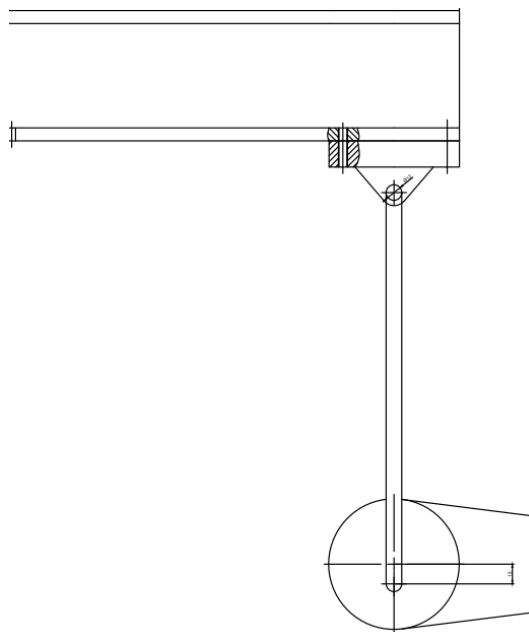
There are three pieces that connects the beam with the rotating disc.

- The bar that transfers the movement between the rotating disc and the beam.

- A piece that connects the bar and the beam in order to allow the rotation in the x axes, so the movement is transferred without any deformation or stress.

- The bolts that connect the pieces.

The main structure of the machine consists of:

- The support platform, the whole machine is supported by this structure.

- Two beams supported by this platform; the beams are connected to a third one that completes the structure.

- The third beam is the one that have the movement. Is connected with a bolt to the two supporting beams. And it's also connected to the rotating disc in the other side.

- The force sensor and the specimens are assembled with the gripping system.

- The motor and the belt that produces the movement.
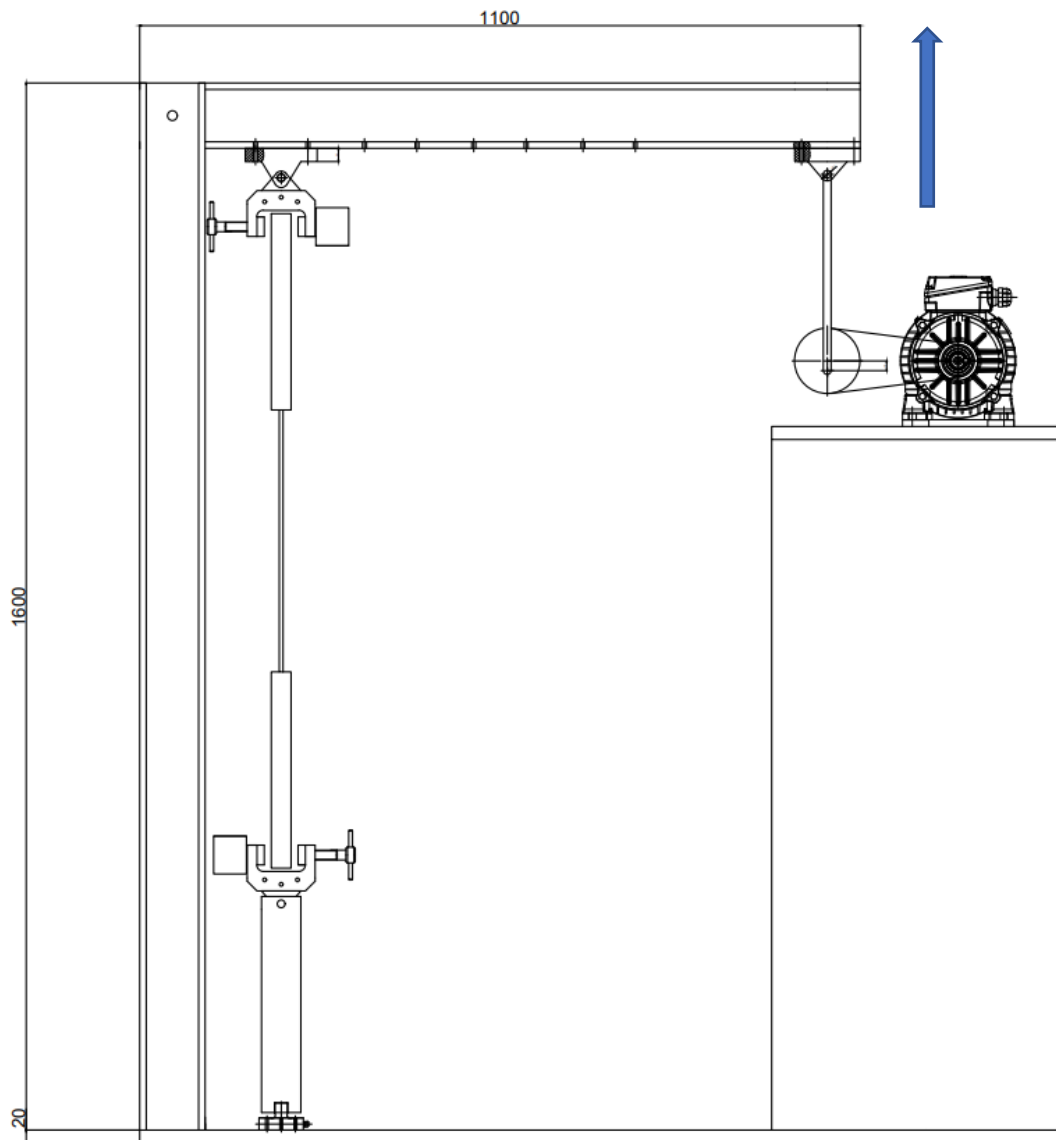
Image11. Schematic image of the machine.

With the information in the images 11 and 12, the movement of the machine is described, that's why this machine is denominated as a control displacement machine. The displacement is applied to the extreme of the beam 3 and is transferred to the entire rotating bar at point D.

The objective of this machine is to perform tests in which the deformation of the specimen varies between 5-20 millimeters. To do this, and using trigonometry, the points at which the amount of the specimens must be placed next to the gripping system have been calculated to obtain the desired displacement, this calculous will be explained later. In this case the machine has four

possible configurations and are the following, displacements applied to the specimen of five, ten, fifteen and twenty millimeters. In the case of being necessary to apply a greater displacement in the future it could be done by adding a configuration more of twenty-five millimeters.

To mount the specimens on the rotation bar, holes have been made that allow adjusting the piece that joins the bar with the gripping system. There are other options such as mounting a guide on the bar that would allow the displacement to adopt the different displacements that were desired, but being complicated and being able to result in a lack of precision since the guide could move, the designed system uses four screws to adjust the position of the specimen in the exact position for the desired displacement and knowing that the position will not vary during the realization of the experiment.

Calculous for the position of the displacement.
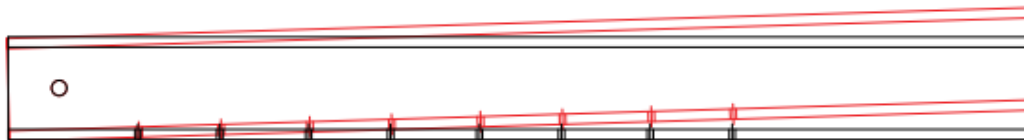
Image 12. Rotating beam in the two positions.

The black position is the starting position of the beam when the cycle starts, and the red one is the maximum displacement position. Using a CAD and applying a displacement of 30 mm to the extreme of the beam in the y axes, the rotation degree of the beam is α=1,72º. This can be also calculated with this formula:

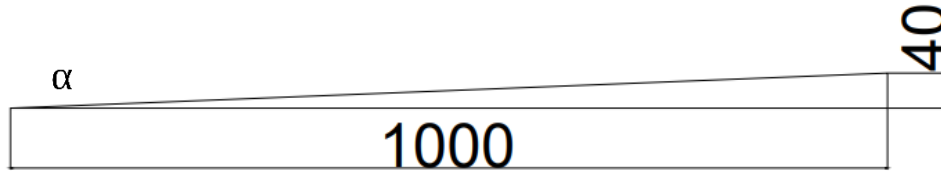*Image13. Rotation of the beam.*

$$sen(\alpha) = {}^{30}/_{1000}$$

$$arcsen(\alpha) = 0.03$$

$$\alpha = 1.719º$$

To calculate the position of the holes that support the connecting piece of the specimens, the following trigonometric relationships are made.

Using again the sen of the angle α we obtain:

1.   To obtain a displacement of 5 mm in the specimen:

$$sen(1.719) = \frac{5}{x}$$

$$x = 166.67 \ mm$$

2.   To obtain a displacement of 10 mm in the specimen:

$$sen(1.719) = \frac{10}{x}$$

$$x = 333.36 \; mm$$

3.   To obtain a displacement of 15 mm in the specimen:

$$sen(1.719) = \frac{15}{x}$$

$$x = 500.03 \; mm$$

4.   To obtain a displacement of 5 mm in the specimen:

$$sen(1.719) = \frac{20}{x}$$

$$x = 666.72 \; mm$$

These are the points where the rotating point of the piece should be located. The piece has the following dimensions.
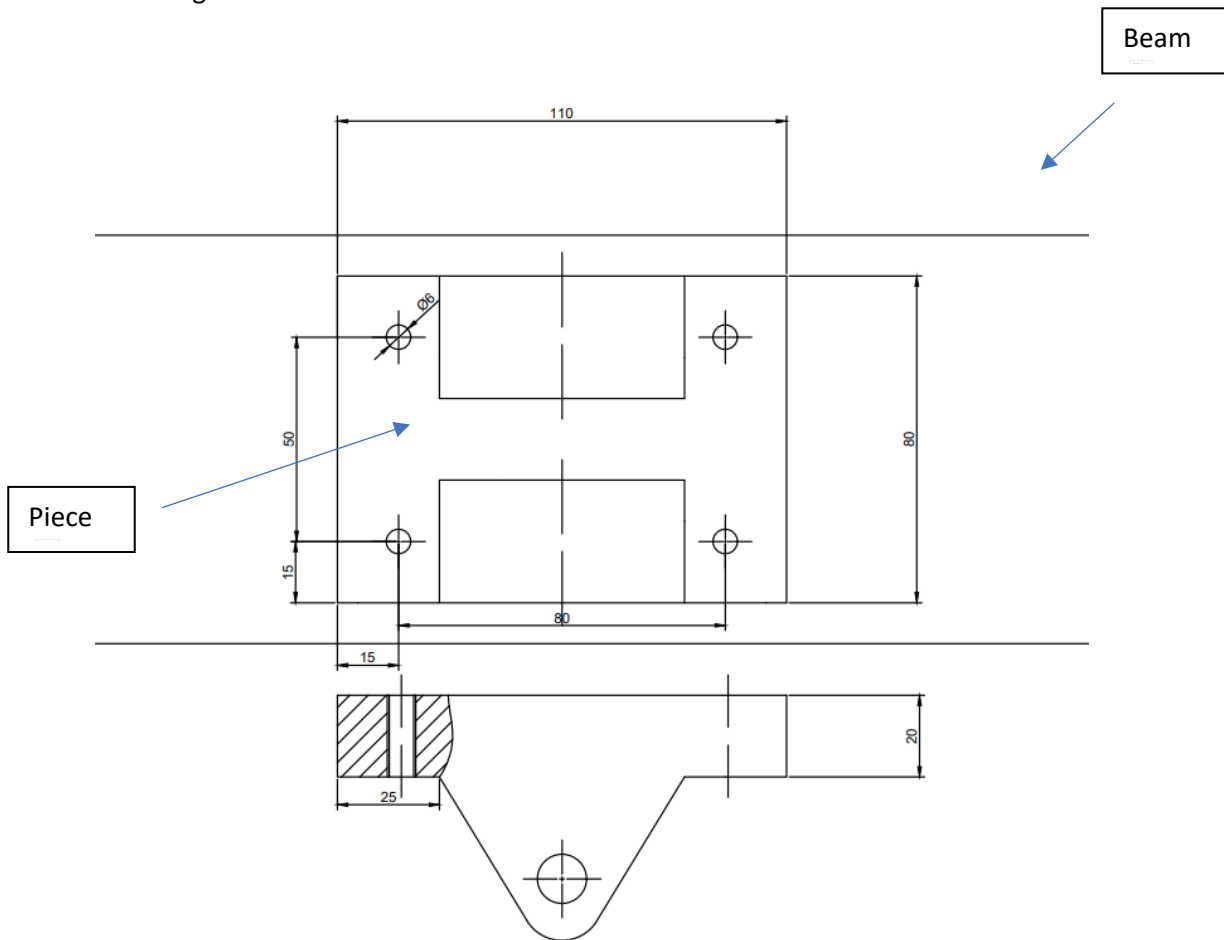
Image14. Piece and beam with the holes.

So, we can calculate the position of the holes to fit with the beam in the correct positions, the piece needs four screws to be full attached to the beam. The calculations for the position of the holes where the following ones:
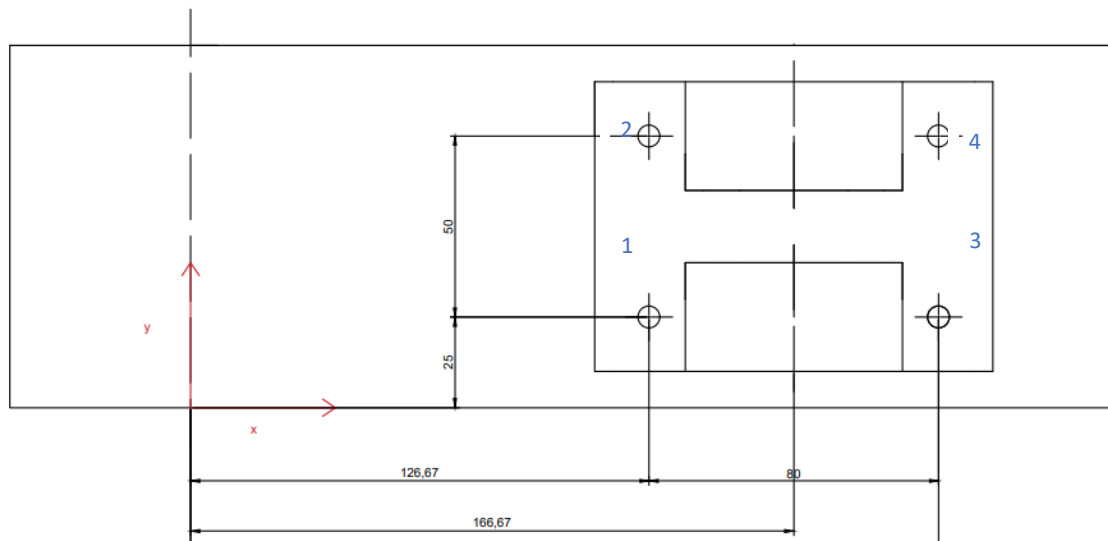
Image15. Position of the holes.

Using as a reference the system of coordinates drawn in red, which is located at the point where the bolt is located on which the bar rotates (y-axis), we obtain the following coordinates for the holes. The distance on the x-axis for the same holes but for a different configuration should be 167.67 millimeters greater than those of the previous configuration.

For the configuration of five millimetres of displacement.

- The hole number one is located in (x, y) = (126.67, 25).

- The hole number two is located in (x, y) = (126.67, 75).

- The hole number three is located in (x, y) = (206.67, 25).

- The hole number four is located in (x, y) = (206.67, 75).

For the configuration of ten millimetres of displacement.

- The hole number one is located in (x, y) = (293.34, 25).

- The hole number two is located in (x, y) = (293.34, 75).

- The hole number three is located in (x, y) = (373.34, 25).

- *The hole number four is located in (x, y) = (373.34, 75).*

For the configuration of fifteen millimetres of displacement.

- *The hole number one is located in (x, y) = (460, 25).*

- *The hole number two is located in (x, y) = (460, 75).*

- *The hole number three is located in (x, y) = (540, 25).*

- *The hole number four is located in (x, y) = (540, 75).*

For the configuration of twenty millimetres of displacement.

- *The hole number one is located in (x, y) = (626.67, 25).*

- *The hole number two is located in (x, y) = (626.67, 75).*

- *The hole number three is located in (x, y) = (706.67, 25).*

- *The hole number four is located in (x, y) = (706.67, 75).*

For the dimensioning of the rotating beam there are more aspects that must be considered. The beam selected is an HEB 100, a standardised beam, with the following dimensions.
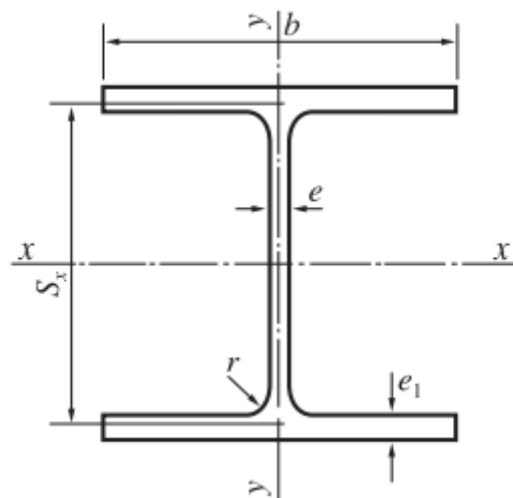
| HEB	Dimensiones (mm)					
	h	b	e	e_1	r	h_1
100	100	100	6	10	12	56
120	120	120	6,5	11	12	74
140	140	140	7	12	12	92
160	160	160	8	13	15	104
180	180	180	8,5	14	15	122

Table 1. Dimensions of the HEB profiles.

For the calculation of the total length of the beam there are two aspects that requires attention. These two aspects were the connexions between the other two beams, and the other connexion with the motor. The length used for the calculations and which squares the system configurations were 1000 millimetres, so to have this effective length is necessary to add some length in these two points.

- The connexion between the three beams:

To allow this connection without changing the inclination degree of the beam and without compromising the stability of the structure is necessary to add 50 millimetres in the start of the beam so this one can be connected in a proper way to the other two.
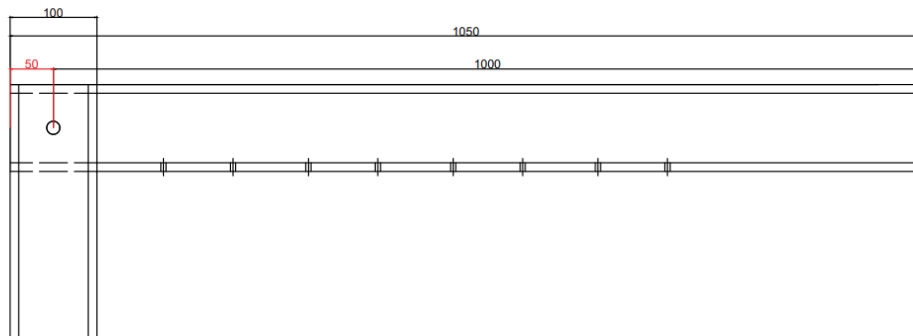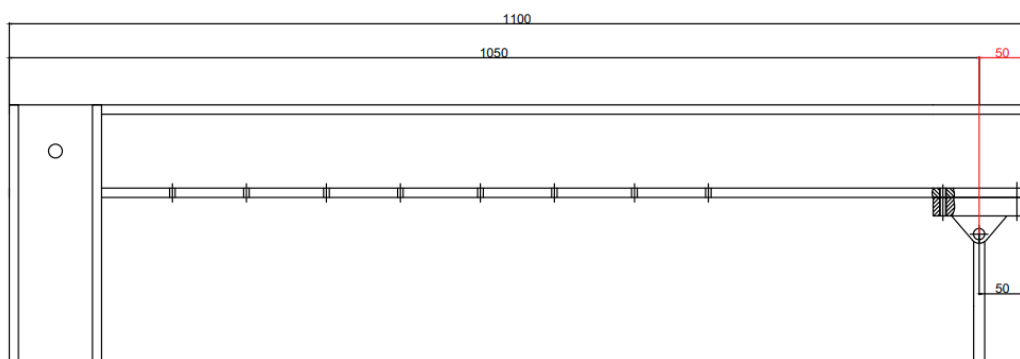
Image17. Connexion between the beams.

In red, the distance of 50 mm that is necessary to add to the beam.

- The connexion with the motor:

The connexion of the beam with the motor is helped with a piece attached to the beam that allow the rotation of the bar that connects the motor and the beam without creating any stress. This piece is quite similar to the one used for the configurations of the deformation but with some differences in the dimensions.


Image 18. Connexion between the rotating beam and the bar.

In red also, the distance of 50 mm needed to add to the beam.

After this the total length of the rotating beam is 1100 mm.

For the design of the supporting structure and the supporting beams, it's necessary to have enough space for the assembly of the specimens, gripping system, and the force sensor. With this configuration we have a space of 1500mm free to add al the pieces that are needed for the testing. This distance can be smaller to optimise the space better but is also a good idea to leave space because in case that any manipulation or change in the pieces of the machine that could require more space. Also, if any reinforcement is needed this space can be used to. In this case to fill this space we have the steel tube that connects the force sensor with the gripping system, in the case that this space is required cutting the length of this pipe will be a simpler solution than increasing the size of the supporting beams.
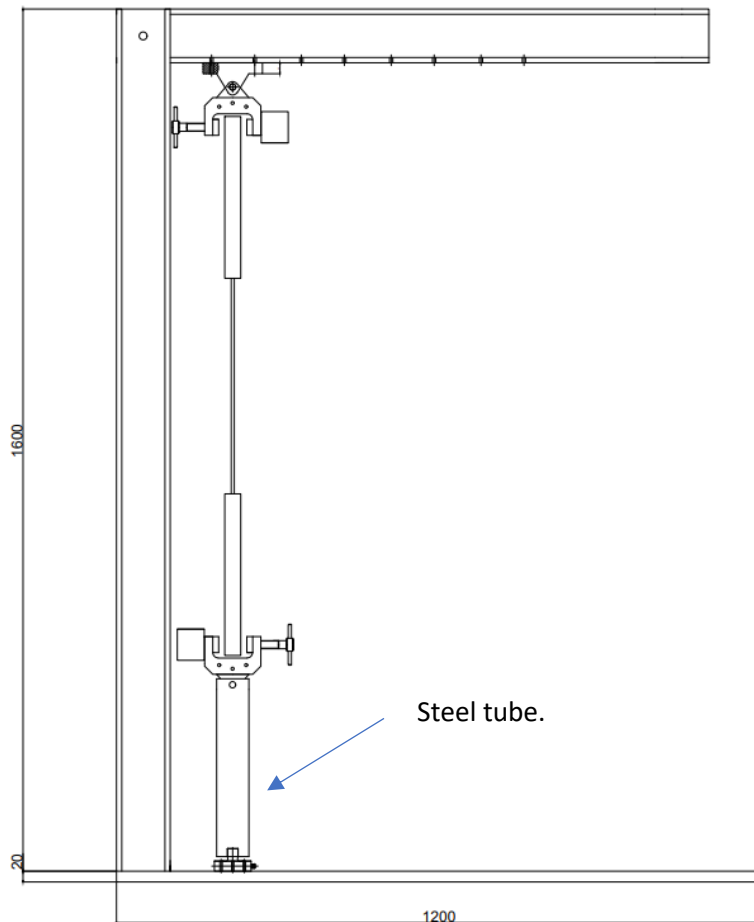
Image19. Schematic image of the structure.

The parts of the machine that remain to be analyzed, excluding the gripping system that will be analyzed at a separate point, are the force sensor and the steel tube.

The force sensor selected is the model KMM40 from the enterprise P.P.H. WObit E.K.J ober. s.c., we need this sensor to know what force is being applied to the specimen at each moment of the test, this is a very important fact, and the sensor must be optimized for the range of values in which it will be used. The maximum force expected on the machine is about 42 KN, this data will be explained on the stress calculations. The data for the selected force sensor:

Właściwości

- Do ogólnego użytku
- Układ mostkowy
- Ściskanie/rozciąganie
- Niski profil
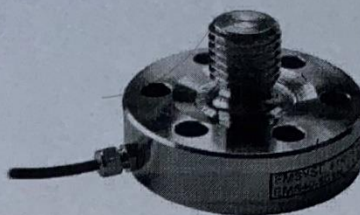
Wymiary

1, 2, 5 kN   10, 20, 50 kN
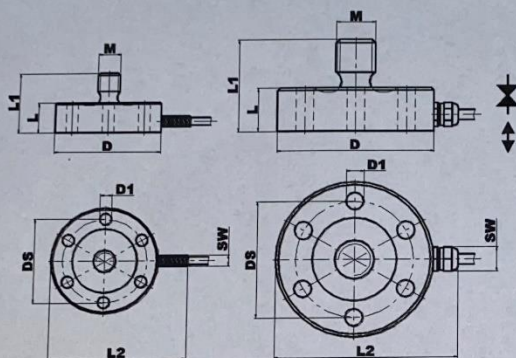
Schemat podłączenia
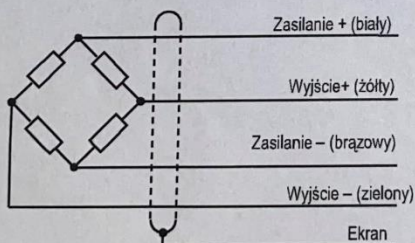
Klasa dokładności	0.5	
Obciążenie znamionowe kN	1, 2, 5	10, 20, 50
Przeciążenie użytkowe Przeciążenie graniczne	150 %F.S. 200 %F.S.	
Wyjście ze stałą charakterystyczną	1.5 mV/V ± 2%	
Tolerancja zera	2 % F.S.	
Nieliniowość, %F.S. Histereza, %F.S.	0.25 0.25	0.5 0.5
Błąd pełzania (30 min)	0,1 %F.S.	
Współczynnik temperatury - punktu zerowego - stałej charakterystycznej	0.1 %F.S./10 °C 0.1 %F.S./10 °C	
Rezystancja wejściowa	380Ω ± 10%	
Rezystancja wyjściowa	350Ω ± 5%	
Rezystancja izolacji	> 5000 MΩ	
Napięcie zasilania - Zalecane - Maksymalne	10 V 15 V	
Zakres temperatury -znamionowy - użytkowy	0 ... + 50 °C - 10 ... + 70 °C	
Stopień ochrony	IP54	
Materiał korpusu	Stal	
Kabel (2 m)	LifYDY 4x0.05	LiYCY 4x0.14

Schemat podłączenia:

Zasilanie + (biały)

Wyjście+ (żółty)

Zasilanie – (brązowy)

Wyjście – (zielony)

Ekran

Obciążenie znamionowe kN	D mm	D1 mm	L mm	L1 mm	L2 mm	M Mm	SW	DS mm
1	38	6x4,2	11	22	46	M8	4	30
2	38	6x4,2	11	22	46	M8	4	30
5	38	6x4,2	11	22	46	M8	4	30
10	50	6x5,2	14	29	58	M10	8	38
20	56	6x6,3	16	34	64	M14	8	42
50	68	6x8,4	19	42	76	M20	8	50

Image20. Force sensor data (Polish Information).

27

As I have already mentioned the maximum force that the machine will be operating is 42 KN, then the selected force sensor is the last one from the table, this one it can measure maximum forces of about 50 KN, this meets the requirements for the operation of the machine. This force sensor is connected to the supporting structure in the floor.

The steel tube connects the force sensor with the gripping system, with this tube the structure is completed. In the point of the connexion with the gripping system the rotation is allowed with a bolt to not have any stress concentrated.
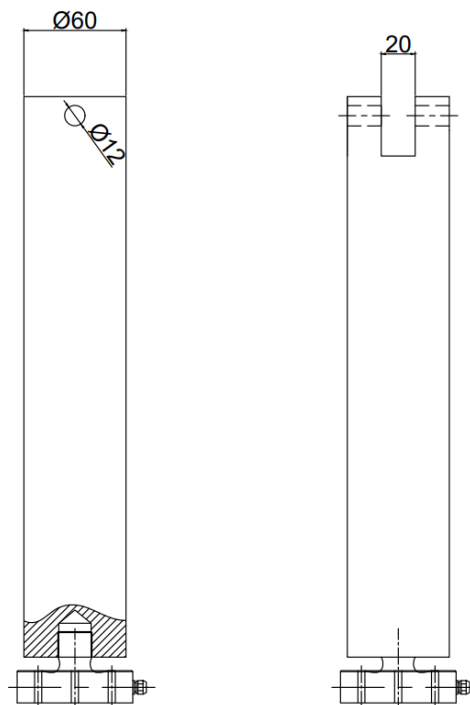
Image21. Steel tube with force sensor.

6. DESIGN OF THE GRIPPING SYSTEM.

The design of the gripping system, it was one of the main problems for the design of the project, since it should meet the sufficient pressure requirements to carry out the tests, and also be compatible with the type of specimens used. There have been several alternatives designed for

the gripping system but finally only one has been selected. The different alternatives have been searched on the websites of manufacturers specialized in the field. It has also been considered the factor that in the gripping system should not concentrate stresses and for the main solution has been modified to allow rotation by two bolts. This is because due to the property of the bar that rotates, it does so with respect to a point, tracing a circular path that despite the fact that the value of the displacement on the perpendicular axis to which the displacement is located is practically zero. The addition of these two connections ensures that no unwanted stress is concentrated in the specimen. One of the possible solutions and one of the most simples were this one:
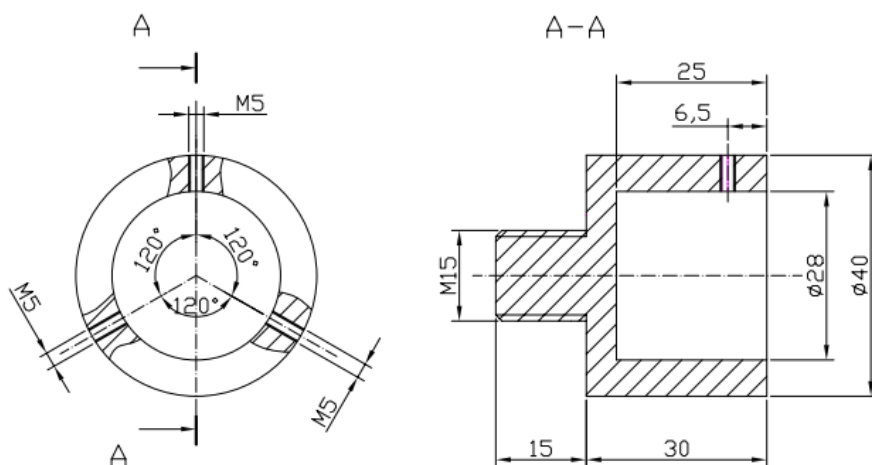
Image22. Alternative 1, griping system.

This solution uses three screws to attach the specimens to the gripping system. The main problem with this solution was that for its use the coating of the specimen must also be drilled to achieve a sufficiently strong hitch. But several factors such as the properties of the material used for the coating, which made it almost certainly break during the test. In addition, during the realization of these holes in the coating of the specimens there was the possibility of

damaging it. In addition to probably losing the ability to perform another type of test with them.

And finally, the use of this type of gripping makes difficult to mount the specimens of the machine and they should need a mechanism to modify the distance between the two hitch points.

The selected solution is the use of the gripping system model MDN-0,6/50- Ko from the company Metrotec, this company performs different types of gags for the performance of traction experiments. These jaws are characterized by being pneumatic and a great aperture to have space for specimens. The selected jaw is the one that meets the dimensions required by the coating of the specimens.
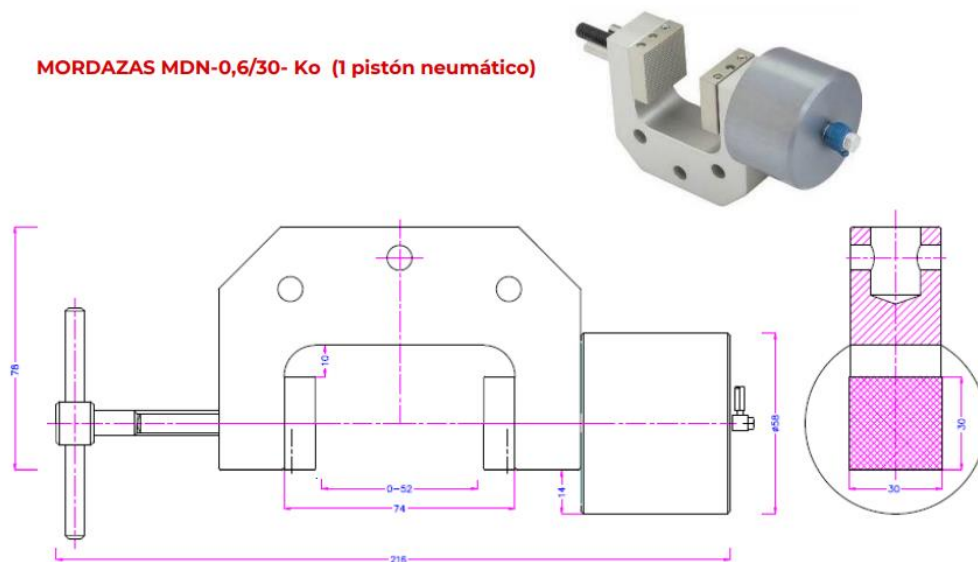
Image23. Selected gripping system.

The main advantages of this gag are the possibility of exchanging specimens easily and without wasting time. The maximum opening of the jaws is 52 millimeters, which meets the size of the coating, which is 30 mm.The mechanical characteristics for the grip are met and the properties of the part are as follows:

• **Fuerza de sujeción:**	1,2 kN a 7 Bar (2,5 kN a 16 Bar con el Compresor UN216)
• **Conexión Neumática:**	Rosca interna M5
• **Cuerpo:**	Aluminio anodizado
• **Mandíbulas:**	Acero niquelado
• **Rango Temperatura:**	0... + 70 ° C (según tipo mandíbulas) Otros rangos bajo pedido
• **Acoplamiento:**	15,9 mm o 20 mm (Otros acoplamientos bajo pedido)
• **Alcance suministro:**	1 par de Mordazas (sin mandíbulas)

Table2. Characteristics of the selected gag.

Traduction of the Table:

1.	Clamping force = 1.2KN to 7 Bar.

2.	Pneumatic Connection = Internal thread M5.

3.	Body = Nickel-plated steel.

4.	The temperature range is 0-70°C.

5.	Coupling 15.9 mm or 20 mm.

6.	Supply range = 1 pair of gags (without jaws).

It is necessary to make a modification to the jaws to as said before allow rotation at the points that connect these with the rest of the system. For this and using the hitch that this has in the upper area we will add a piece that has a hole through which to pass the bolt that connects the gripping system with the rest of the structure in the two required points. The jaws can be

changed in order to have a better grip if the planar ones don't have enough grip due to the circular section of the specimens coating, the company have a stock of different types of jaws.

The final structure of the gripping system will look like this:
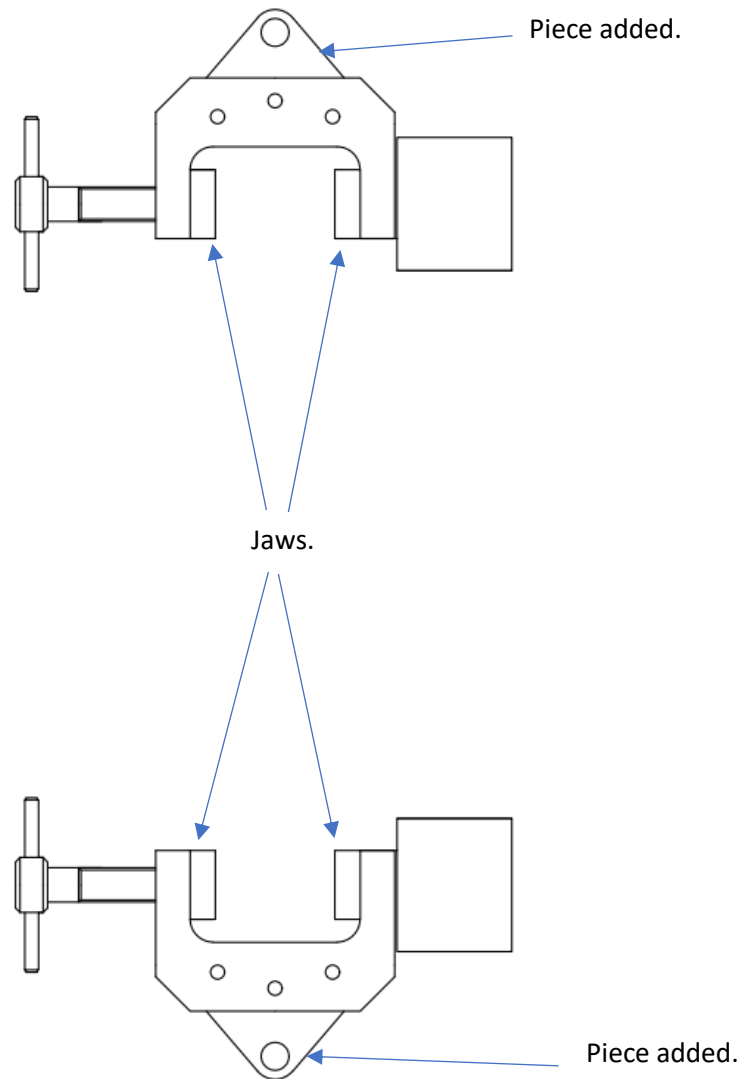
Image 24. Gripping system.

7. NUMERICAL ANALYSIS – KINEMATIC AND STRESS CALCULATIONS.

7.1 Kinematic calculations.

For the kinematic calculations, one of the main objectives is the possibility of carrying out studies using different cycle speeds. To do this and performing the following calculations we can obtain a table with the possible speeds at which the fatigue test can be performed and the angular speed necessary on the motor to obtain this. The angular speed of the motor is transferred to the rotating wheel by a pulley, with this we can obtain a formula to make a relation between both angular speeds. The formula:
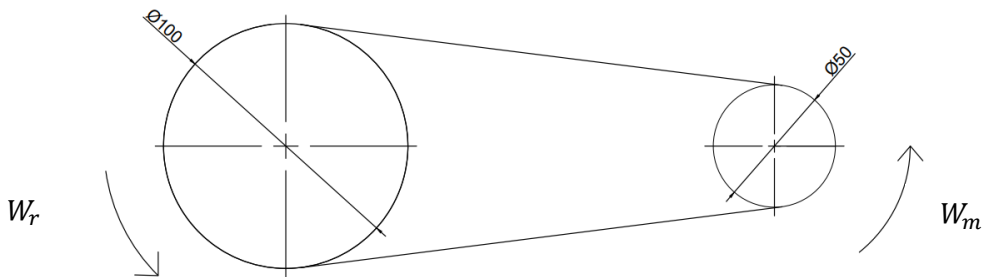
Image25. Pulley between motor and rotating wheel.

$$W_r * d_r = W_m * d_m$$

$$f = {}^1\!/_T$$

$$T = {}^{2\pi}\!/_W$$

With the values of the frequency that we will need on the rotating wheel and the previous formulas we can calculate the following table to know the required velocity on the motor to preform the test we want.

Wheel			Motor		
Frequency(Hz)	Period(s)	W (rad/s)	W(rad/s)	Period(s)	Frequency(Hz)

3,00	0,333	18,850	37,699	0,167	6,00
2,75	0,364	17,279	34,558	0,182	5,50
2,50	0,400	15,708	31,416	0,200	5,00
2,25	0,444	14,137	28,274	0,222	4,50
2,00	0,500	12,566	25,133	0,250	4,00
1,75	0,571	10,996	21,991	0,286	3,50
1,50	0,667	9,425	18,850	0,333	3,00
1,25	0,800	7,854	15,708	0,400	2,50
1,00	1,000	6,283	12,566	0,500	2,00
0,75	1,333	4,712	9,425	0,667	1,50
0,50	2,000	3,142	6,283	1,000	1,00
0,25	4,000	1,571	3,142	2,000	0,50

Table3. Angular speeds in the motor and the rotating wheel.

The average speed of the motor is between 10-50 Hz and the maximum speed to be achieved during the tests is about 2 Hz for Polymeric composites. To adjust the speed of the motor to the speed required an inverter will be used. This device allows us to change the frequency which the engine works. An inverter is a device that changes or transforms an input voltage of direct current to a symmetrical output voltage (sine, square or triangular) of alternating current, with the magnitude and frequency desired by the user or designer.

The linear speed and the acceleration on the point of the joint between the wheel and the bar that transfers the movement to the machine, in this case the velocity will be calculated for the point of the maximum frequency of the test 2Hz, and it can be calculated with the following formula:

$$\vec{v}_B = \vec{v}_A + \vec{\omega}_3 \wedge \vec{r}_{AB}$$

$$\vec{a}_B = \vec{a}_A - \omega_3^2\,\vec{r}_{AB} + \vec{\alpha}_3 \wedge \vec{r}_{AB}$$
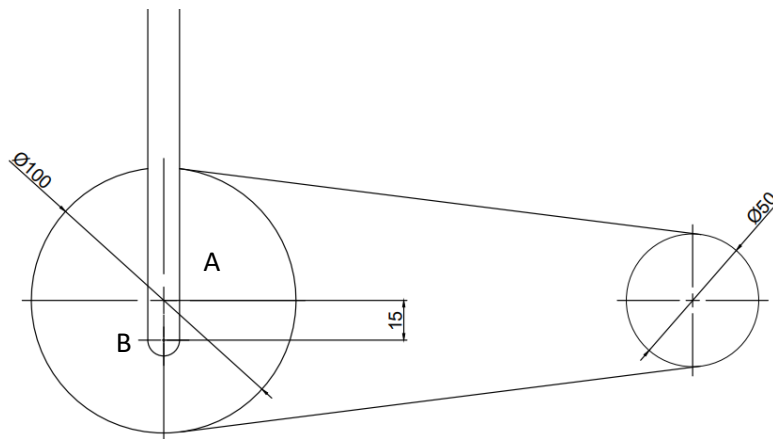
Image26. Connexion between rotating wheel and the bar.

$$W3 = Wr$$

$$V_a = a_3 = 0$$

$$Vb = W_3 * r_{AB} = 4\pi * 15 \text{ mm} = 188,5 \text{ mm/s}$$

7.2 Stress calculations.

This part is the most extensive and the one that has taken the most time of the design put of

the complexity to model the structure of the machine in a software that would allow to check

the behavior of the structure before the loads produced during the test. Among the different

possible options to perform the modeling, the Siemens NX program is the one chosen to

perform the static simulation of the model. The main objective of the simulation of the test is

to obtain the stresses that will form in the structure of the machine and the pieces that form

this one, to analyze the behavior at breakage especially the von Misses stress and the

displacements product of these stresss.

7.2.1 Data from the composite bars testing.

In this point will be presented all the information given to analyze the samples and the requirements of the test.

- Young modulus,

for BFRP bars average Young modulus from three samples: 49,5 GPa.

For GFRP bars average Young modulus from three samples: 44,06 Gpa.

- Samples.

Sample	Surface preparation	Diameter$[mm]$	$L[mm]$	$L_a[mm]$	$E[GPa]$
BFRP1	Primer + quartz sand (0.1-0.3mm)	6	400	300	Pull-out
GFRP2	Primer	6	400	300	**43.4**
GFRP3	Primer + quartz sand (0.3-0.6mm)	6	400	300	**44.0**
GFRP4	Primer + quartz sand (0.1-0.3mm)	6	400	300	Pull-out
BFRP5	Sandblasting	6	400	300	**48.3**
BFRP6	Primer + quartz sand (0.3-0.6mm)	6	400	300	**49.9**
BFRP7	Primer	6	400	300	**50.2**
GFRP8	Sandblasting	6	400	300	**44.8**
GFRP9	Primer + quartz sand (0.1-0.3mm)	10	300	500	Pull-out

Table 4. Samples dimensions and characteristics.

- σ(Mpa)/ε(%) graphics.
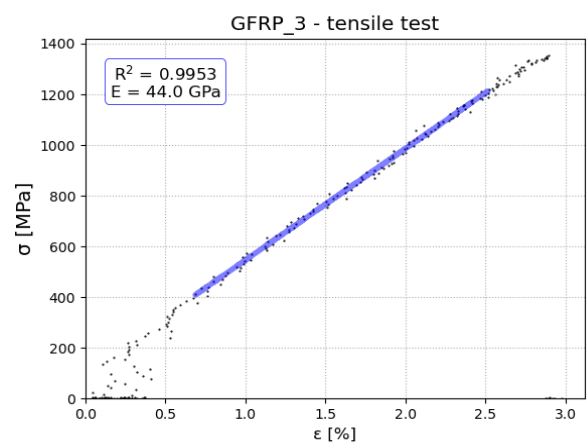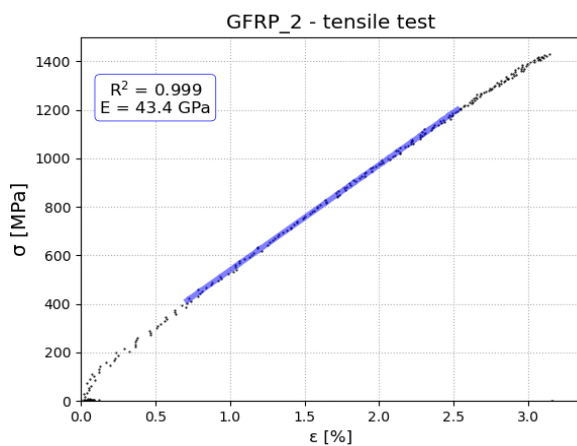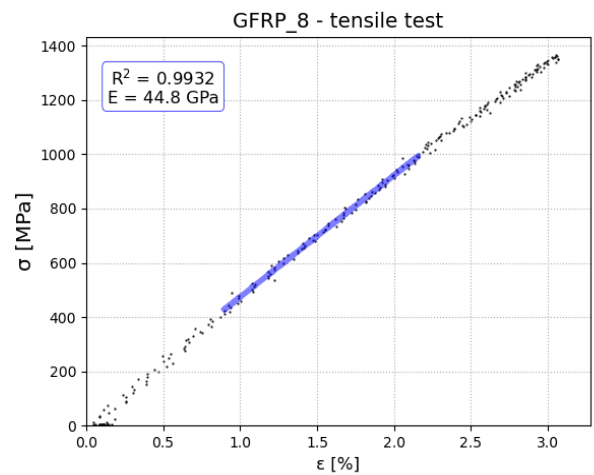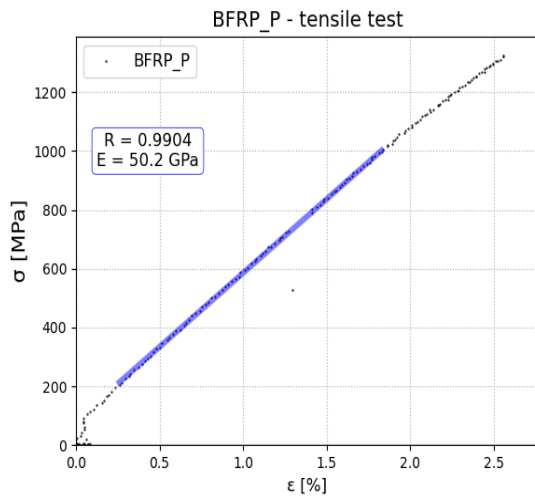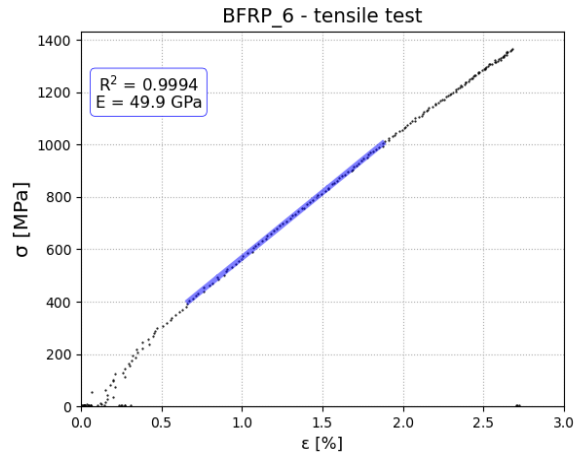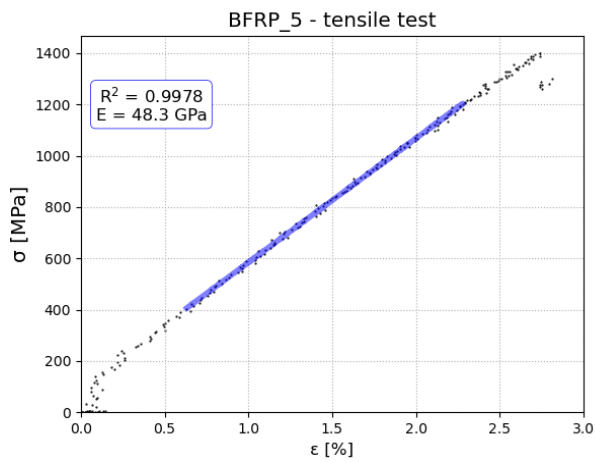
Image27. Tensile test graphics.

From these graphics, the information we can obtain is the force needed to obtain these stresss. The maximum stress of this tables is about 1500 MPa, from this data we can obtain the maximum force that will be applied to the specimens during the test. This data is very important because is necessary to perform the analysis to the structure in Nx.

$$\sigma = {}^{F}\!/_{A}$$

$$F = \sigma * A$$

The Area formula for a circle is:

$$A = \pi * r^2$$

With this we obtain:

$$F = 1500 \ ^N/_{mm^2} * \pi * 3^2 \ mm^2 = 42411 \ N$$

Every piece will be checked to resist this force without exceeding the yield strength.

7.2.2 Nx Siemens.

NX is Siemens Digital Industries Software's solution for the digital development of 3D products for industry, with high-performance integrated applications. For design: advanced solutions for conceptual design, 3D modeling and documentation, for simulation: multidisciplinary simulations for analysis of structural, motion, thermal, flow, Multiphysics and optimization data and for manufacturing: complete parts manufacturing solutions for tool, machinery and quality inspections.

Nx is one of the industry's most powerful, flexible and innovative product development solution, NX for Design, delivers the features, performance and capabilities needed to help you get your product to market faster than ever. NX for Design allows you to market products directly and for the first time using more virtual product models and fewer physical prototypes, which are more expensive. All this results in an increase in profits in the market, a reduction in development costs and an improvement in the quality of products.

The previous knowledge for the use of the program were those acquired during the laboratory of the subject Finite Elements Method taught by the Wroclaw University of Science and Technology during the winter semester.

7.2.3   Modelling and results.

At this point the procedure followed for the modeling of the machine will be developed step by step. The forces and constrains applied to the model will also be specified. Finally, the results for the configuration of materials and final dimensions will be presented. The analysis of the structure will be preformed with the use of the assembly FEM, to do this we have to follow the following steps:

7.2.3.1 Modelling of the structure.

1.   Modelling of the beams.

The first stage of the process is to create every .prt part in an individual model.

Modelling of HEB100_1 and HEB100_2, the two supporting beams are equal, so the process of the modelling will be repeated.
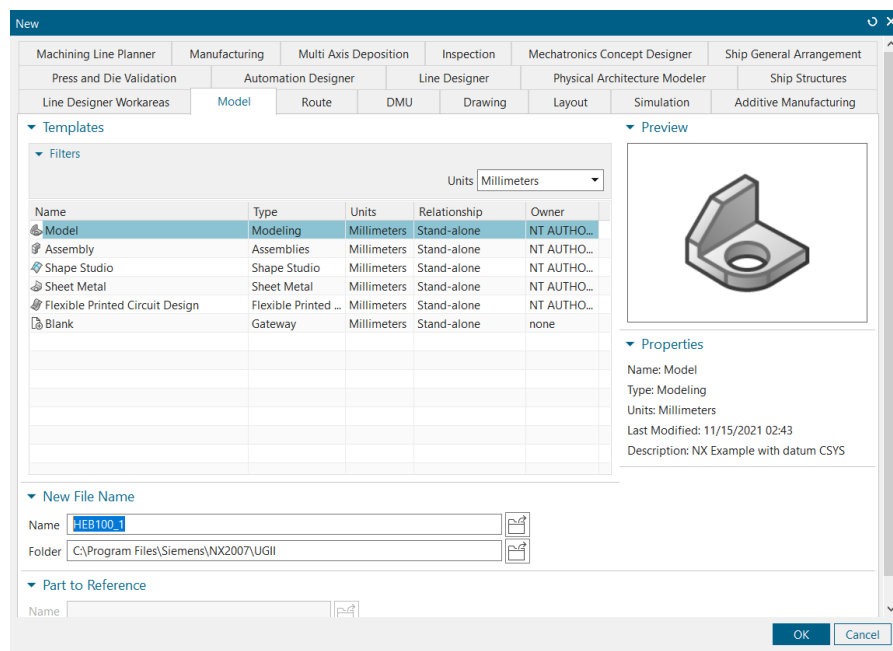
Image28. Create a new model Nx.

First of all, press New and select the type of file Model.
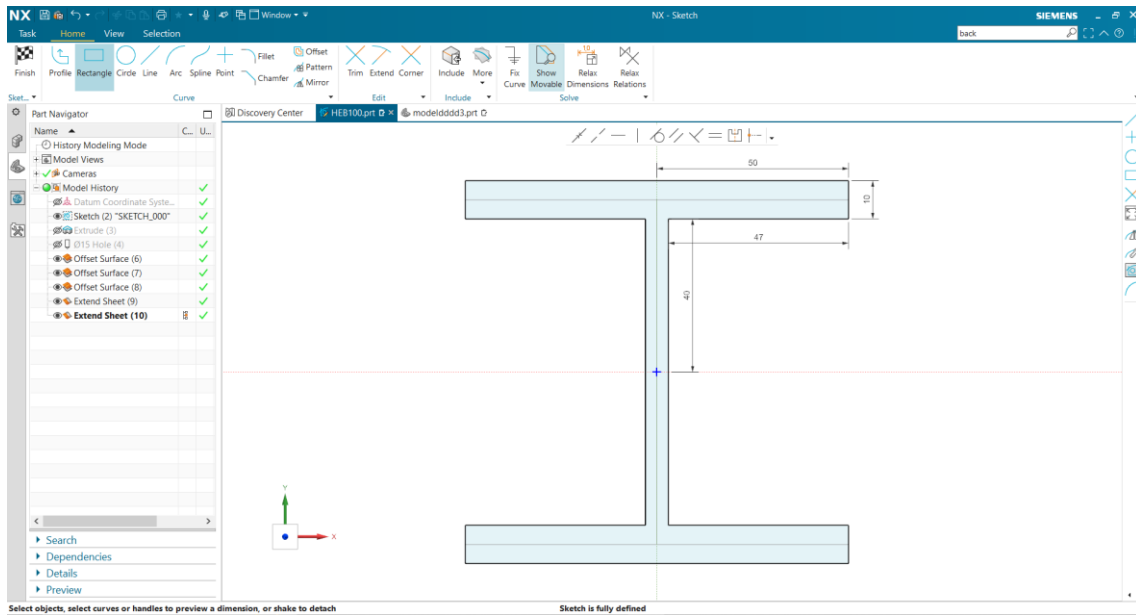
Image 29. HEB100 Sketch.

Then extrude the sketch to obtain the 3D model, in this case 1600mm.
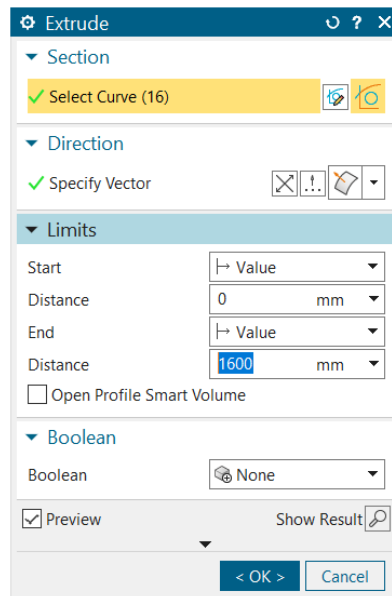
Image 30. Extrude.

Create the hole for the bolt connexion between beams, in this case the hole diameter is 15mm.
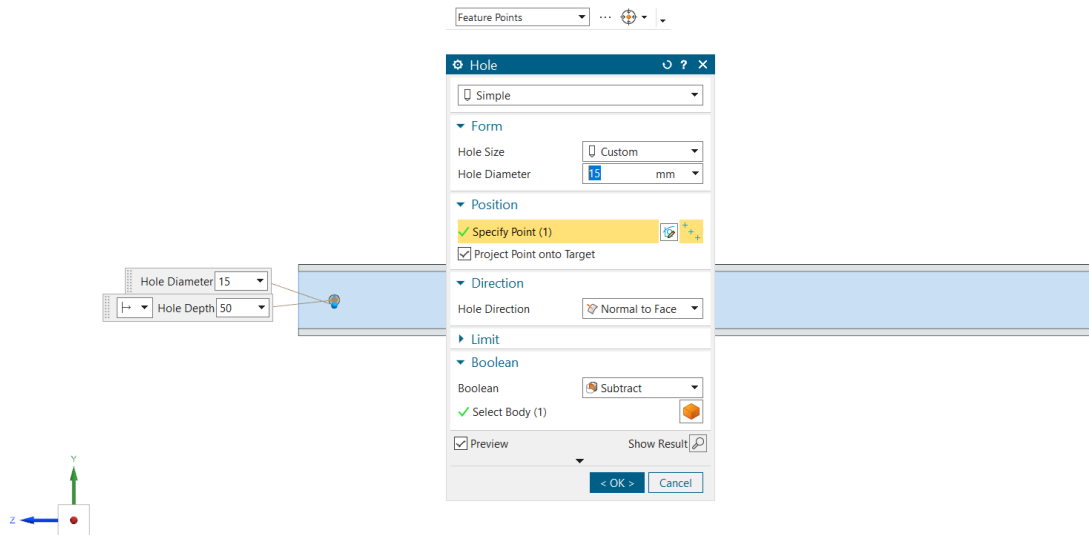
Image31. Bolt hole.

For the analysis of physical elements, we will use 2D elements, to be able to use this we must create offset faces to the faces previously created during the extrude process. These offset faces must be found in the middle of the structure. It will be done by using the offset Surface and extend sheet commands, the result will be as follows:
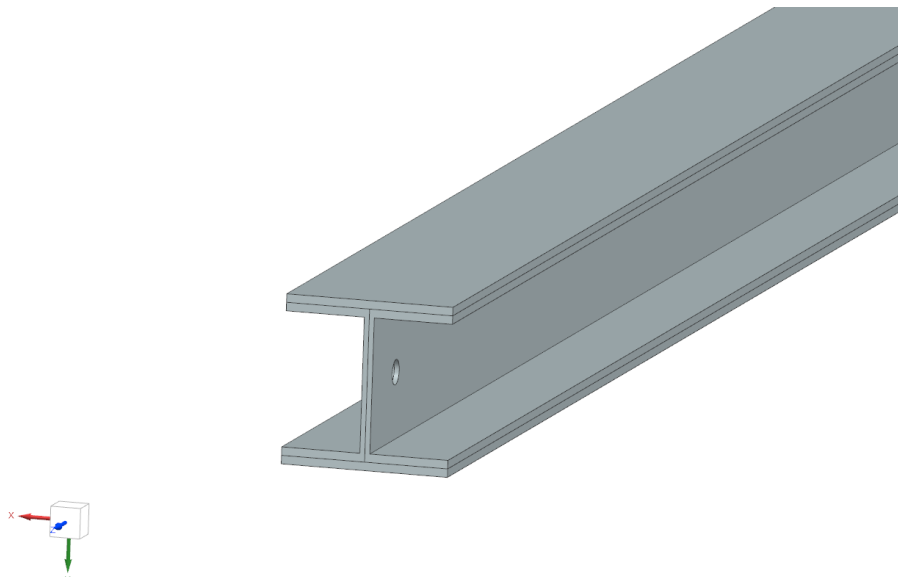
Image32. 2D modelling.

After this we will go to the Pre/Post .fem application to apply a material to the created parts and create the mesh to divide the body into finite elements.

The modelling of the third beam is really similar to the process of the first two ones, so as not to repeat the modeling process again, the differences will be explained. In the extrude command the length of the bar will be 1100 mm and additionally the holes that allow the coupling of the piece for the four configurations of the model must be created, the positions of these holes are explained in chapter 5.2. The final result of the bar is this one.
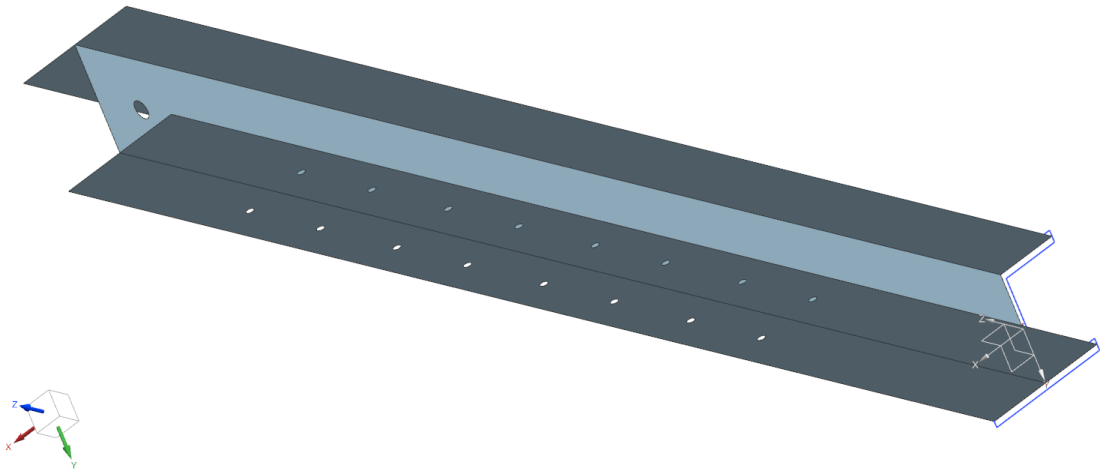
Image33. HEB100_3 model.

2.   FEM model creation.

The first thing that must be done is create the physical properties of the 2D collectors, for this the type of PSHELL element will be used, the characteristics of the material that we must add to these elements are material, in this case Steel and the thickness of the material. In the three beams we have two different thickness 10mm and 6mm so we will create a physical property for each case.
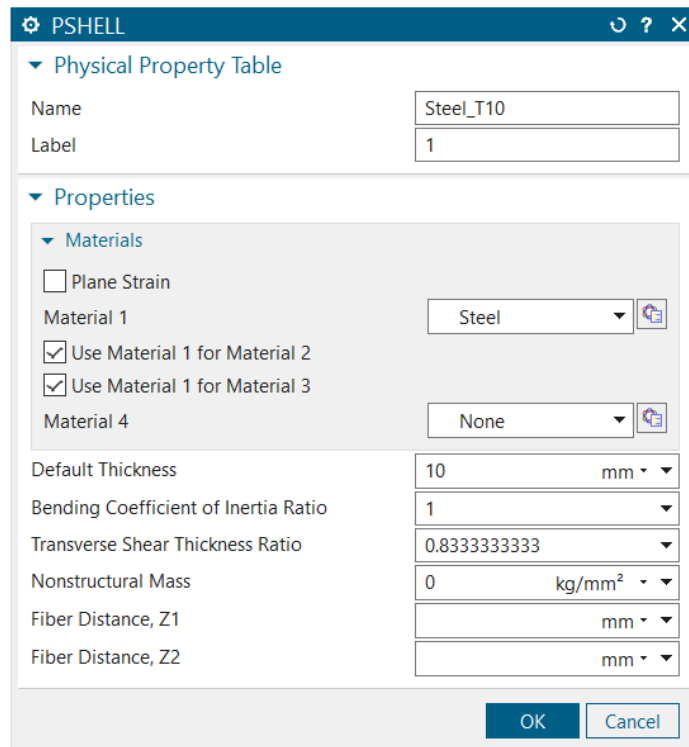
Image34. PSHELL Physical Property creation.

The next step is creating the mesh collector.
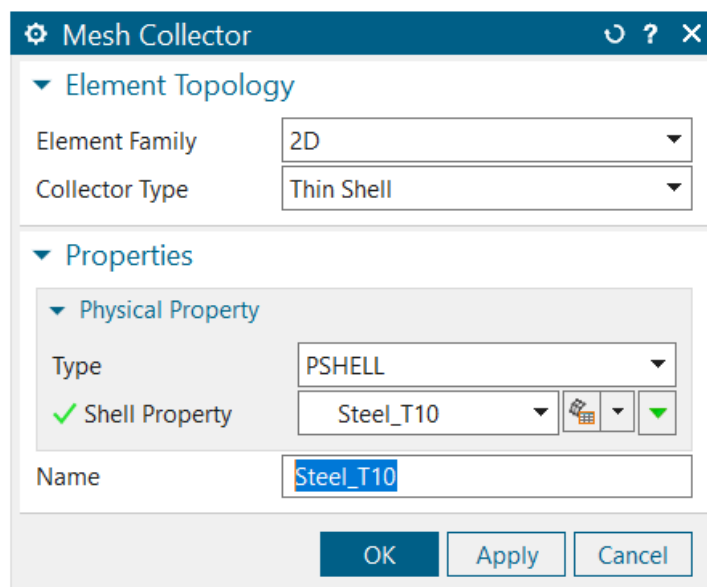
Image35. Mesh collector creation.

Once we have the properties of the material we can create the mesh, which will have the

following characteristics.

43
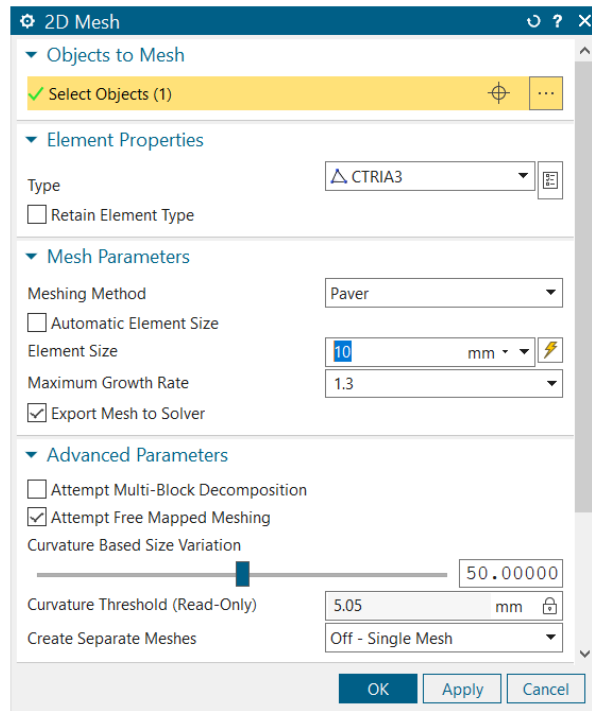
Image36. Mesh properties.

The type of mesh used for the faces that doesn't have a hole will be the CQUAD4 to perform better results, and the CTRIA3 for the surfaces that have a circular hole so they are not allowed to use the CQUAD4 mesh. Different simulations have been carried out using element size smaller and using CQAD8 and CTRIA6 obtaining similar results. This type of mesh uses more nodes which makes the time it takes the computer to perform the simulation is very high, that is why it has been decided to use the configuration found in *image 35* for every face of the beams that forms the whole structure. A large number of simulations have to be carried out to check each of the configurations of the system and the practically zero difference in the results means that this configuration has finally been used. It is necessary to check that each mesh is in the appropriate collector, cause this indicates the thickness of the material an important property during the test.
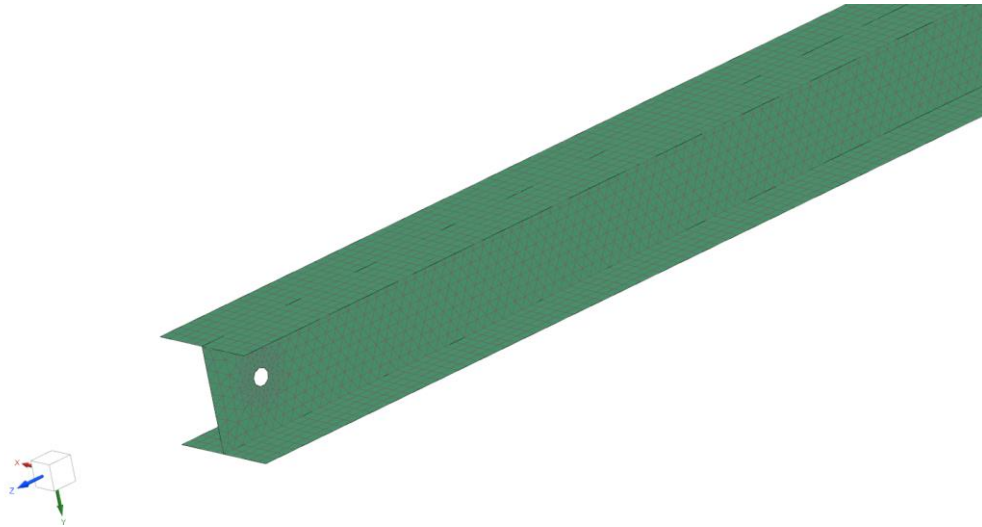
Image37. Final mesh for HEB100_1 and HEB100_2.

Then we have to repeat this process for the other two beams, and the only difference is during the creation of the HEB100_3, the mesh used for the surface with the holes for the coupling will have a CTRIA3 mesh instead of CQUAD4.

3.   Assembly creation.

A new work must be created, in this case when we are on the screen of the image27, we will select assembly. When we have created the model we must load each of the three bars from the .prt files by the command add a component. Once we have the three beams loaded, with the assembly constrains command we will collocate each of the beams in their position and the final result will look like this.
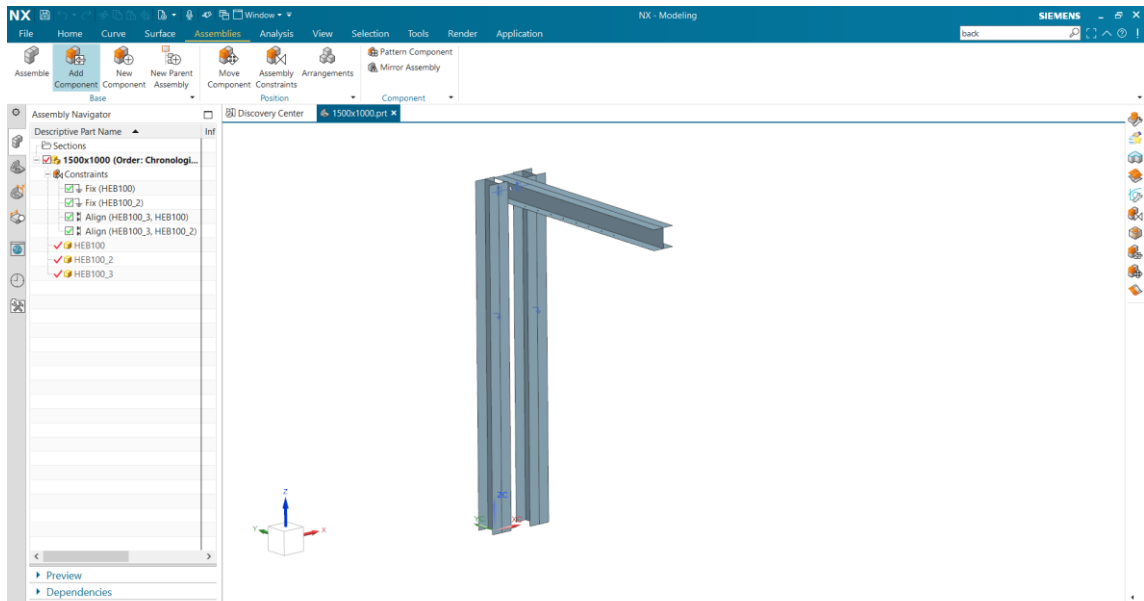
Image38. Assembly structure.
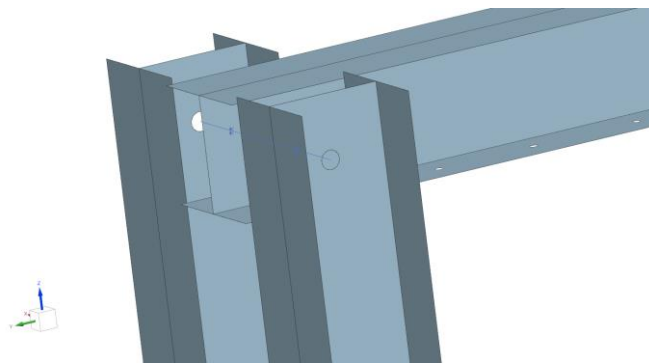
Image39. Align constrain between the three holes.

The constrains used were two fixed constrains, one to each supporting beam to have these beams attached to the ground, and two align constrains between the holes to have all the beams in the needed position.

4.   Creation of the assembly FEM.

In the Application Pre/Post we must select the option to create a new assembly FEM. Once we are at this point, we must load the beam structures again, in a similar way to the previous step. But this time, the .fem files of each of the beams that appear in the position placed in the

previous step will be loaded. Clicking with the right bottom on the mouse here select map existing and add the three beams.
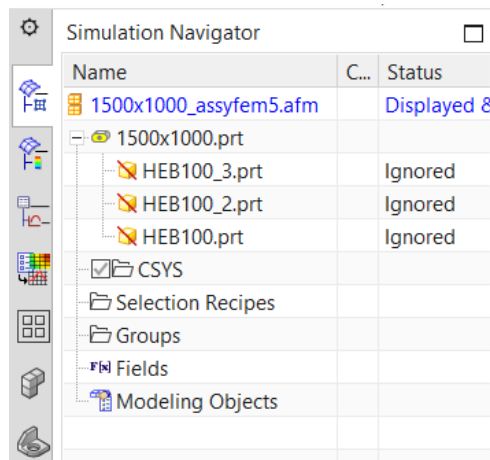
Image40. Map existing command.
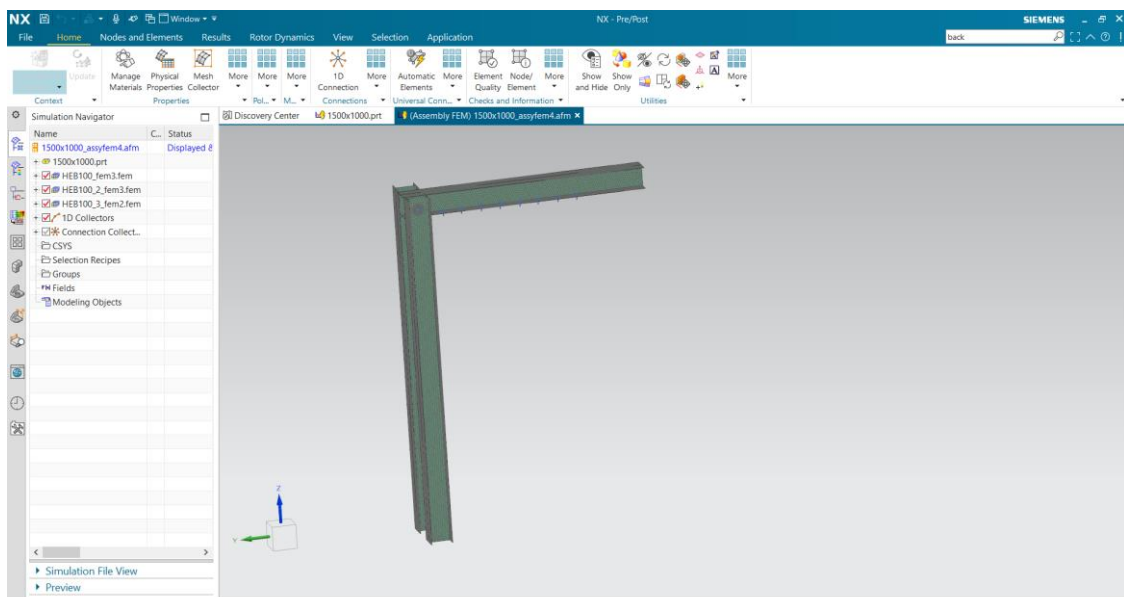
Image41. Assembly FEM loaded.

The next step, which has been more complicated to perform has been the way to connect the three beams so that the rotation around the bolt was allowed so that during the simulation any inappropriate stress of that type of connexion were accumulated at the point of the connection. It is also necessary to ensure that the loads are transferred to the supporting and not only concentrated on the rotating beam.

The first steep is creating the physical properties of the Bolt.
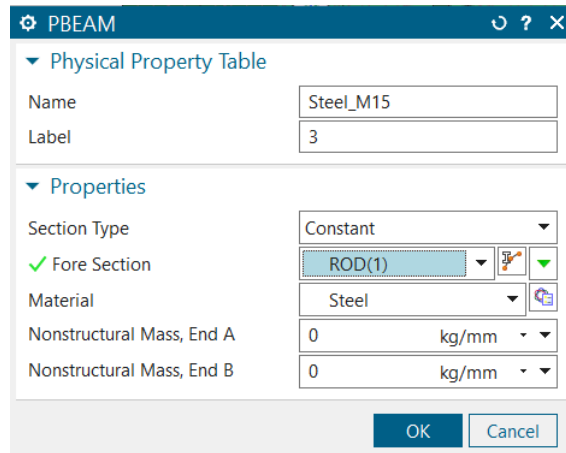
Image42. Physical properties of the connector.

The type of element selected is PBEAM, the fore section ROD(1) is a circle of 15 mm diameter
that simulates the bolt and the material selected is steel. After this, create the mesh collector
for the PBEAM element with the name of bolt.

The next steep is the creation of the RBE2 element on the three holes, using a 1D connection
point to edge in each hole. With this we concentrate the hole on a point on the middle of this
one. With this we are able to create the Bolt connexion between the three holes.
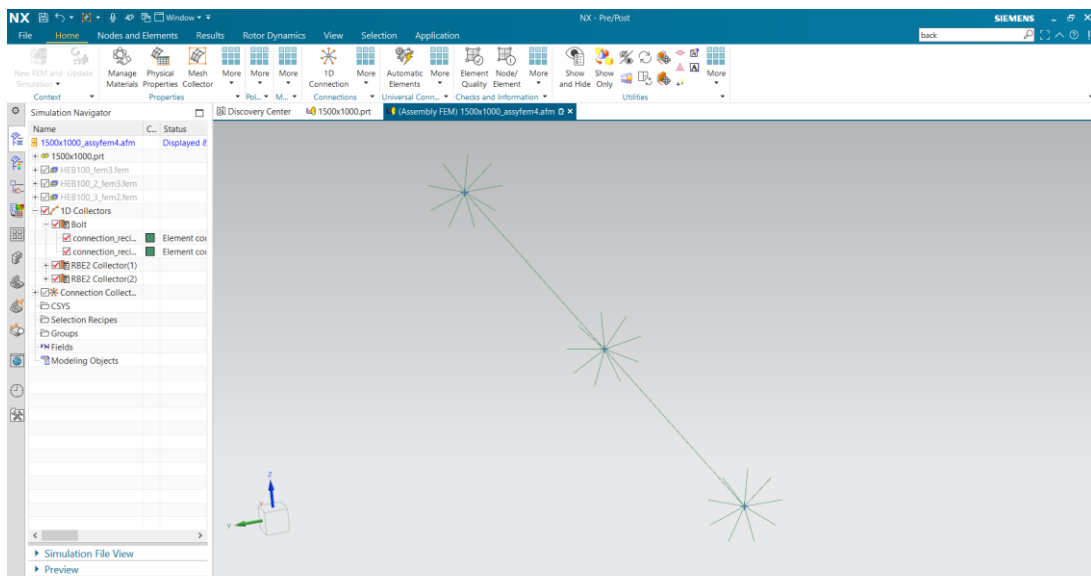
Image43. RBE2 and Bolt connection.

If we deactivate the meshes for a moment we can clearly see the two connections made. On the one hand the three "stars" are the RBE2 connection that makes it possible to make the next connection. The lines that join the three points are the connection created as a bolt that will allow the three bars to be connected and the loads to be transferred. But is necessary another step before starting the simulation. As I have already said it's necessary to allow the rotation in the axe of the bolt because CBEAM elements transfer all 6 DOFs in their nodes. To make rotation possible, it's necessary to edit the mesh associated data of the bolt connections. And add pin flags on the required DOF, in this case the DOF needed is the rotation around x axe.
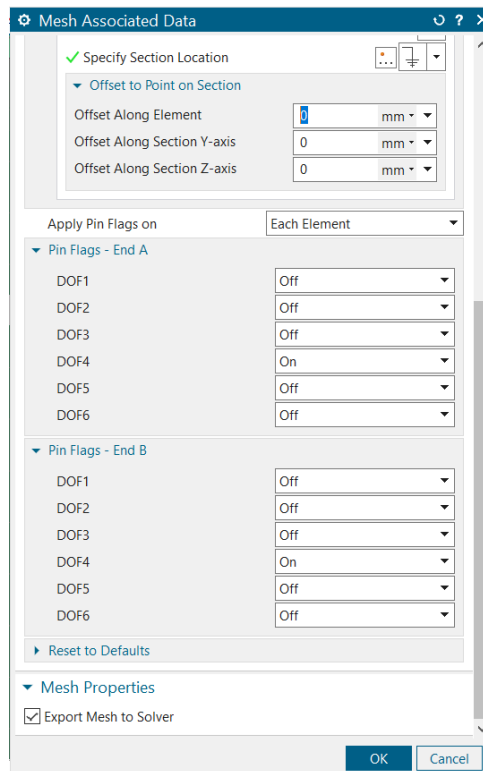
Image44. Pin flags on the bolt connexion.

The last thing required, before starting the simulation phase is the creation of RBE2 elements on the holes of the rotating beam, because a force will be placed on that holes and creating the RBE2 element is a simple way to connect the force to the hole.

5.   Simulation.

This is the last phase before obtaining the results, at this point we must add the constrains and the forces. The simulation of each of the configurations will be carried out to study the stresses in each of the different cases that the machine can be found, Also, an additional simulation will be carried out in which only the constrains that hold the supporting beams with the ground and the displacement of 30 mm at the end of the rotating beam will be included to study the behavior of the bolt connection between beams.

- Constrains, they will be active in every simulation, they are applied on the orange edges of the pictures.

The full attachment in the connexion of the beam with the floor.
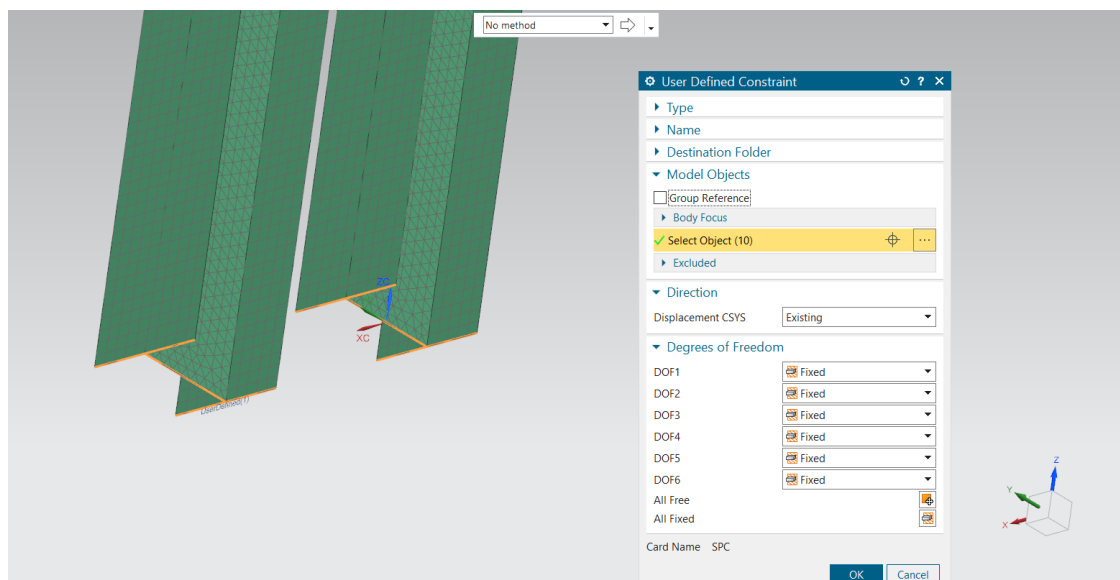
Image45. Full attachment constrain.

The second constrain, is a control displacement that simulates the movement provided by the motor in the extreme of the rotating beam.
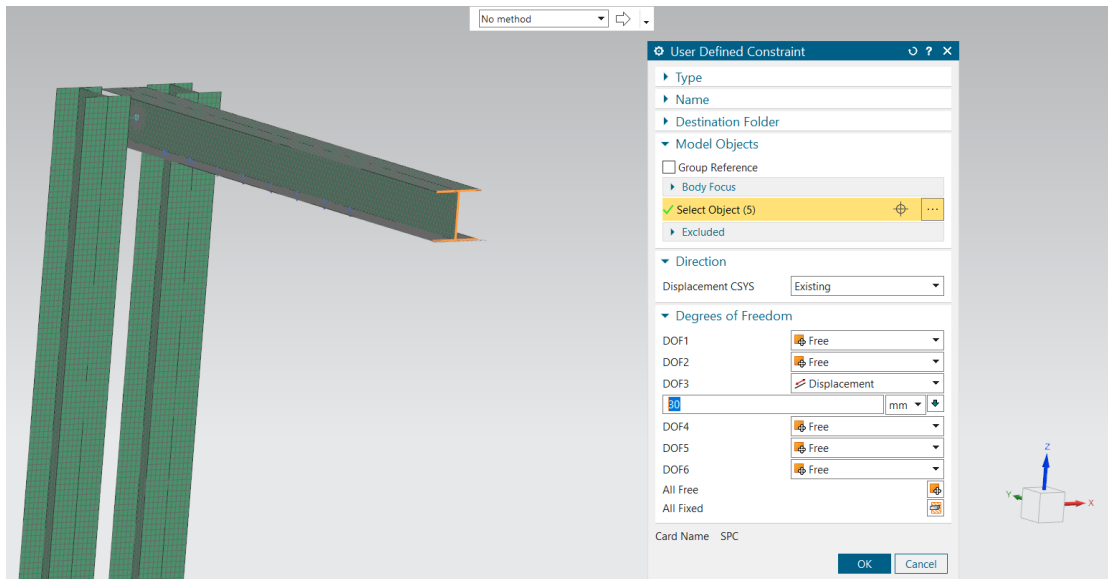
Image 46. Displacement constrains.

In this case the displacement of the beam is 30 mm on the z axe (DOF3).

- Forces.

For the simulation of each of the configurations the reaction force is in the position of the mechanism where the specimens are mounted, the maximum force required in the system was calculated in point 7.2.1, this is 42KN. This force is transmitted to the bar by the piece that is attached to it by four screws, during the placement of the force a simplification will be made. The total force will be divided into four and applied at the points corresponding to the holes where the piece should be attached transmitting the force to the beam. This is done due to the complexity to connect all the parts in the same assembly, the other pieces will be analyzed in a separate simulation.

In every simulation the forces are changed into the next position.
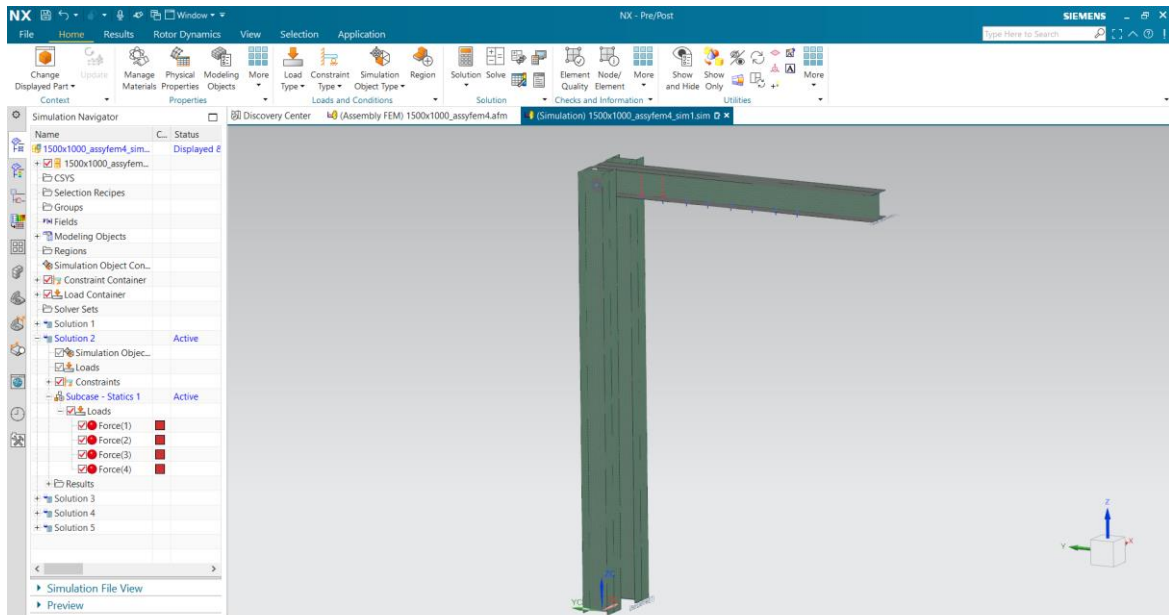
Image47. Screen before testing.

6.   Results.

At this point the results obtained during the static simulation of the bar will be developed and studied.

First of all, to check the correct operation of the machine, the parameters related to the movement of the mechanism must be checked to verify that it works in compliance with the theoretical principles presented in point 5.2 regarding the relative movement of the rotating bar. The following images will present both the displacement of the bar and its angle of rotation around the bolt.
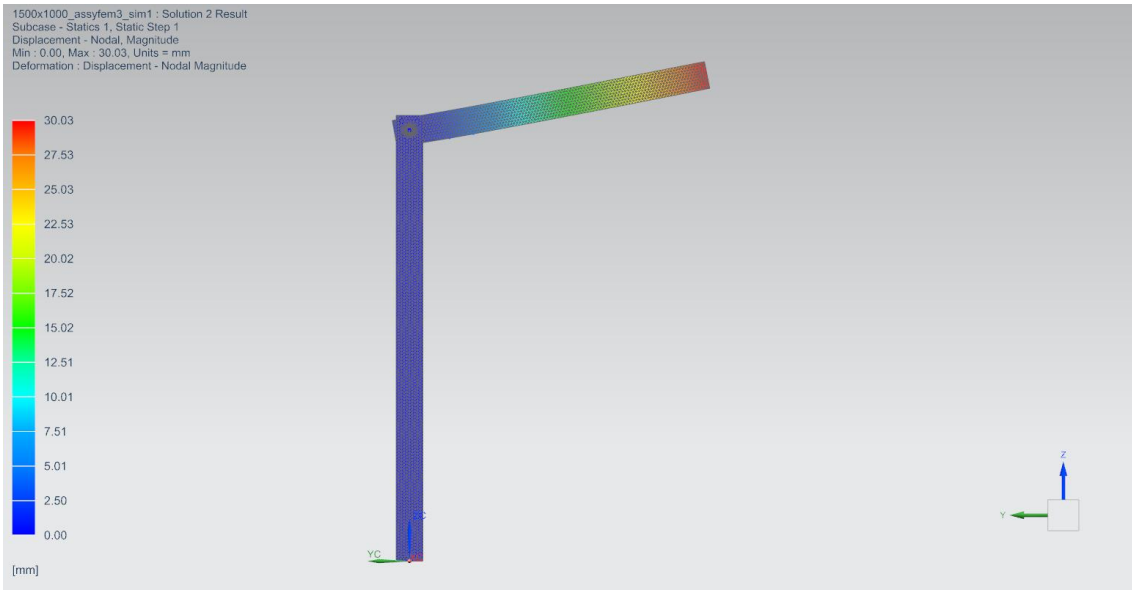
Image48. Displacement.
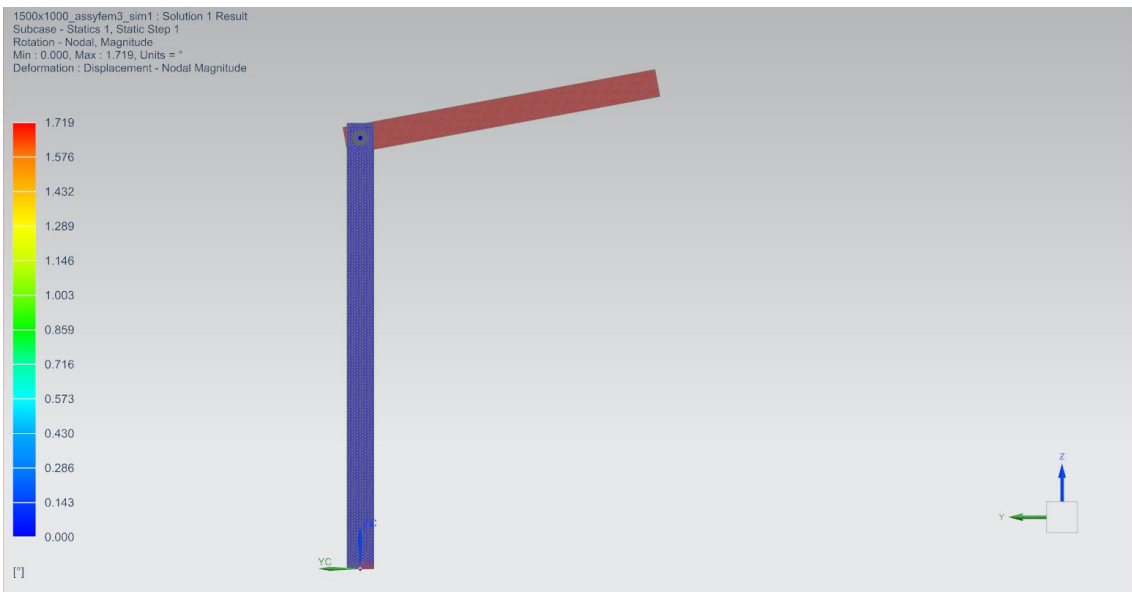
Image49. Rotation.

From these two images we can verify that the data calculated for the displacement and rotation angle of the beam are correct, for the displacement the difference of 0.03 mm is due to the characteristic movement of the bar itself that rotates around a bolt making a circular trajectory. Being the constrain added a fixed displacement on the z axis and regarding the movement of the rotating beam. This is the explanation of why this minimal difference

between the displacement applied by the constrain and that obtained in the results. Since to meet the constrain of a displacement of 30 mm on the z axis the bar has to move a little more since it makes a circular trajectory and cannot move parallel to the axis (that is, without tilting)

The angle obtained in image 48 is the same as that obtained during the theoretical calculations.

- Configuration 0, no loads.

This simulation has been carried out to check the behavior of the union by means of the CBEAM element between the three bars, the image has been zoomed in at the point of the union since it is the point where the stress concentrator is located, this will be the case for all the configurations that will be presented below, because this is always the point where the maximum stress is located. In addition, the behavior of the rotating will be studied at the point where the biggest stress is concentrated (it is will always be between the holes of the simulated configuration). All these simulations are carried out with the aim of checking the behavior of the bar during the test and to check if the mechanical conditions of the material are able to withstand the test process. To do this and using the value of the Von-mises maximum stress, the following formula will be applied to know the safety coefficient.

$$\sigma_{VM} = \frac{Yield\ strenght}{\gamma}$$

$$\gamma = Safety\ coefficient$$
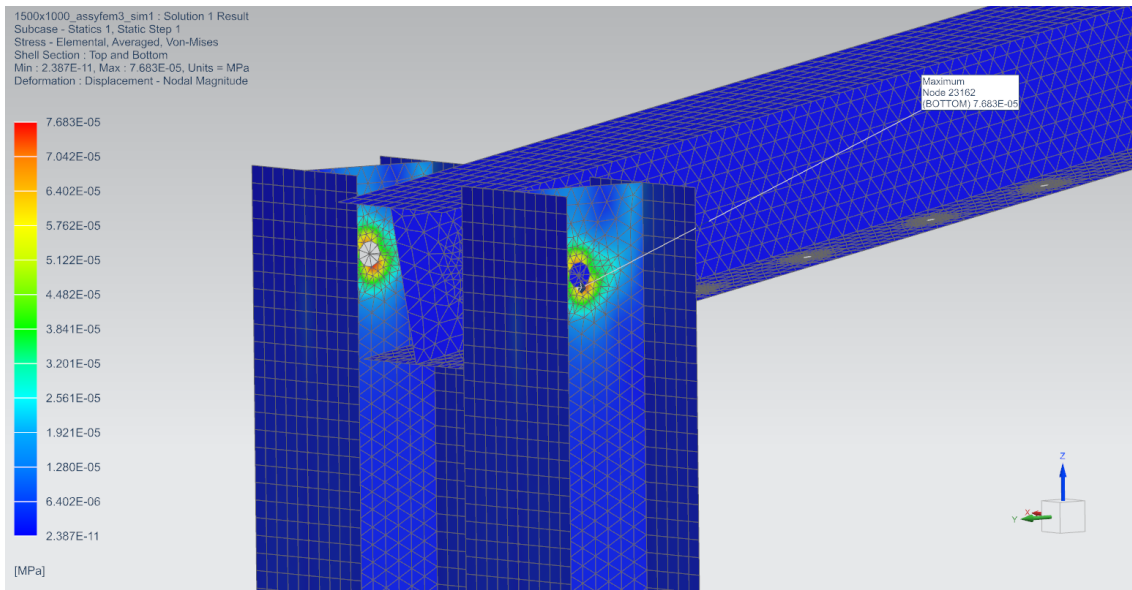
Image50. Von-mises subcase 0.

From this image you can see how the loads caused by the displacement are transmitted to the support bars fulfilling the objective of the type of union made. In addition, these stresses have very low values, including the maximum stress. The value of the maximum stress is of the order of 10^-5 MPa a practically zero stress. This is due to the configuration of the connector element allowing rotation around the x-axis, the system will be at a dynamic simulation point, in which the movement described by the machine is not restricted.

When we apply the necessary forces this simulation will again be a static simulation since then the rotation beam will meet the forces in the opposite direction to its movement hindering the movement and creating stresses in the system.

- Configuration 1, 5 mm displacement.

This is the most critical point in terms of the stresses created in the support bars. Since the loads are at the point closest to the joint, the stress absorbed by the rotating bar is lower and therefore most of the load is transferred to the support bars at the bolt connection.
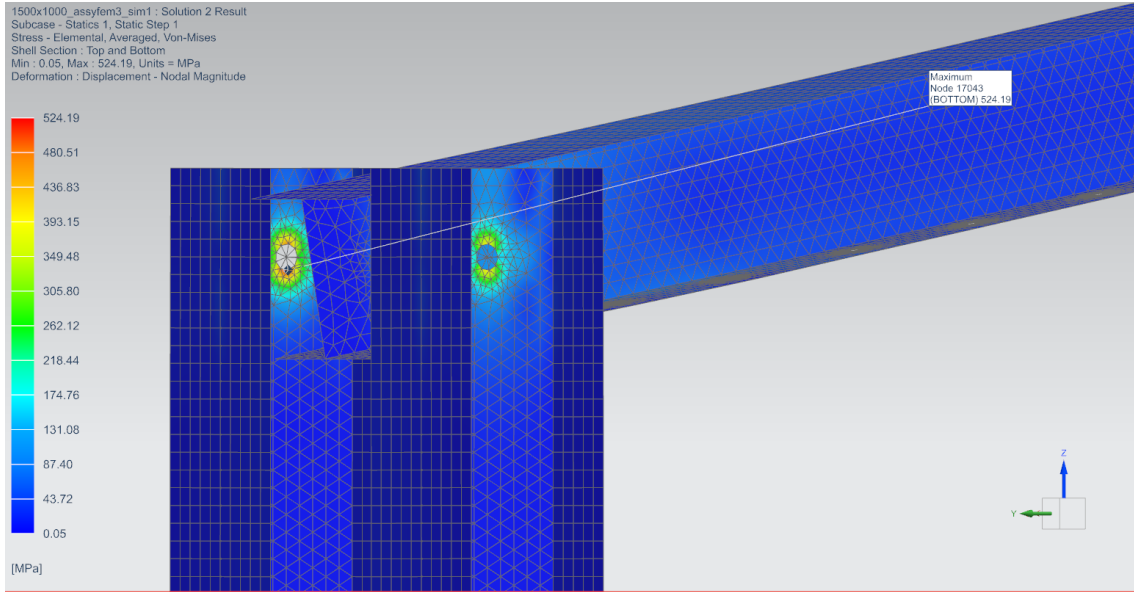
Image51. Von-mises displacement 5 mm.

In the image you can see how it is fulfilled that the maximum stress is concentrated in the support bar at the inner point of the bar (although only one of the faces of each of the bars is seen, both bars provide the same results on the faces) the maximum Von Mises load for this configuration is 524.19 MPa a high result that will be discussed later.
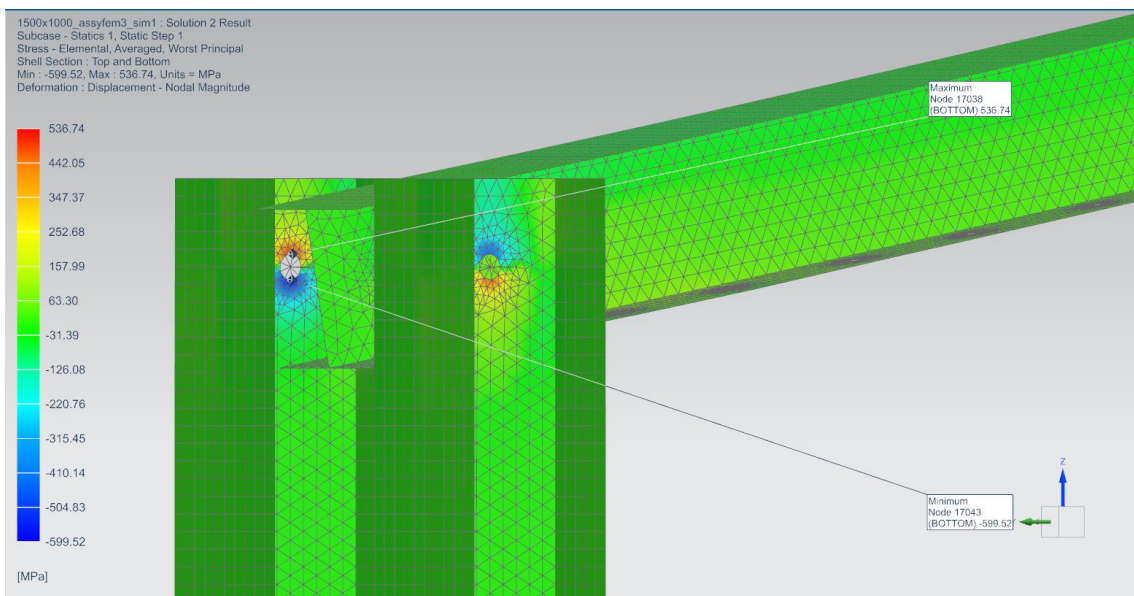
Image52. Worst principal displacement 5 mm.

Looking at the Worst principal stress to observe the behavior of the structure that is mostly at a neutral value of 0MPa, however at the junction point of the bars it is observed how the hole is between two states of stress. Compression in the lower zone and traction in the upper zone.
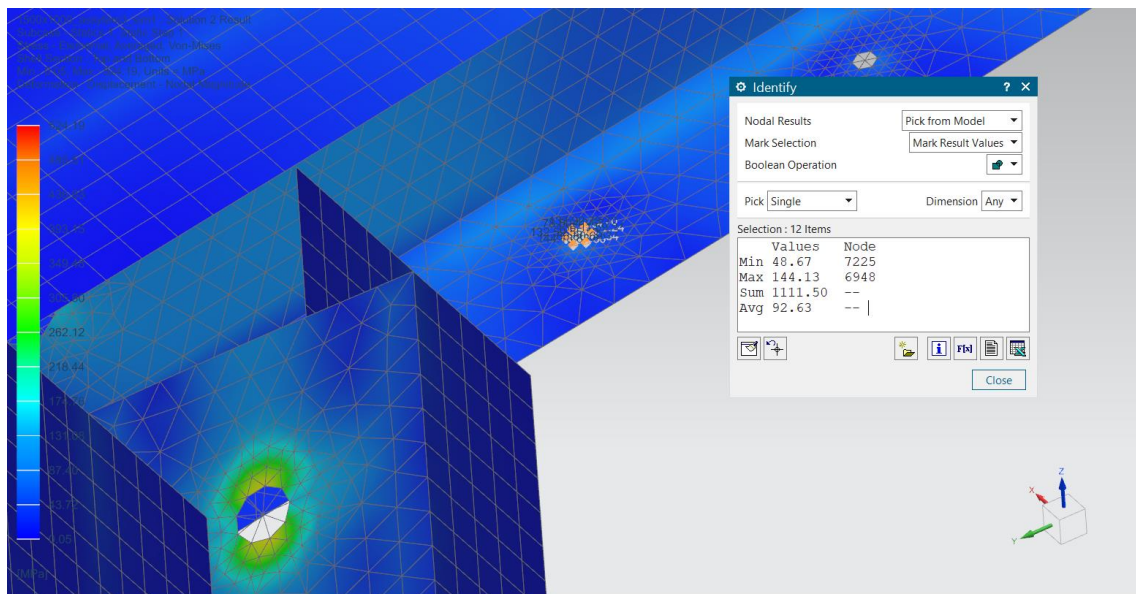
Image53. Von-misses next to the hole 5 mm displacement.

Using the identify results command we analyze the stress values in the nodes that form the hole where the force is applied, we obtain a maximum stress of 144MPa and an average stress of 92.63 Mpa.

- Configuration 2, 10 mm displacement.
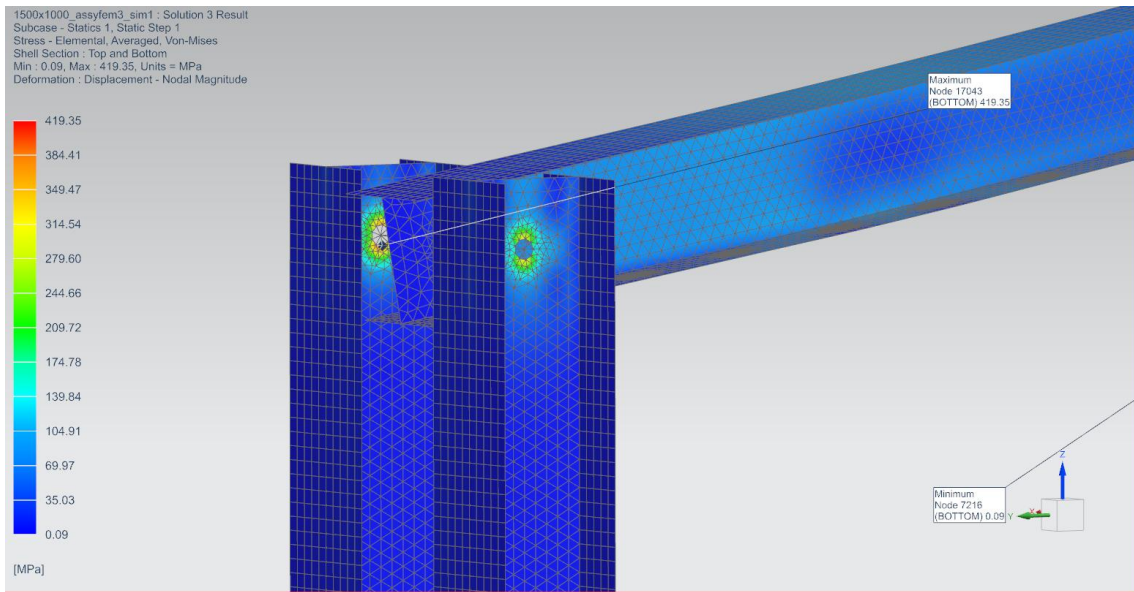
Image54. Von-Mises displacement 10mm.

Here we can see that the maximum stress is still concentrated at the same point and in this

case, it is 419.35 MPa a bit lower than that of the previous configuration since the forces are

further away from the union.
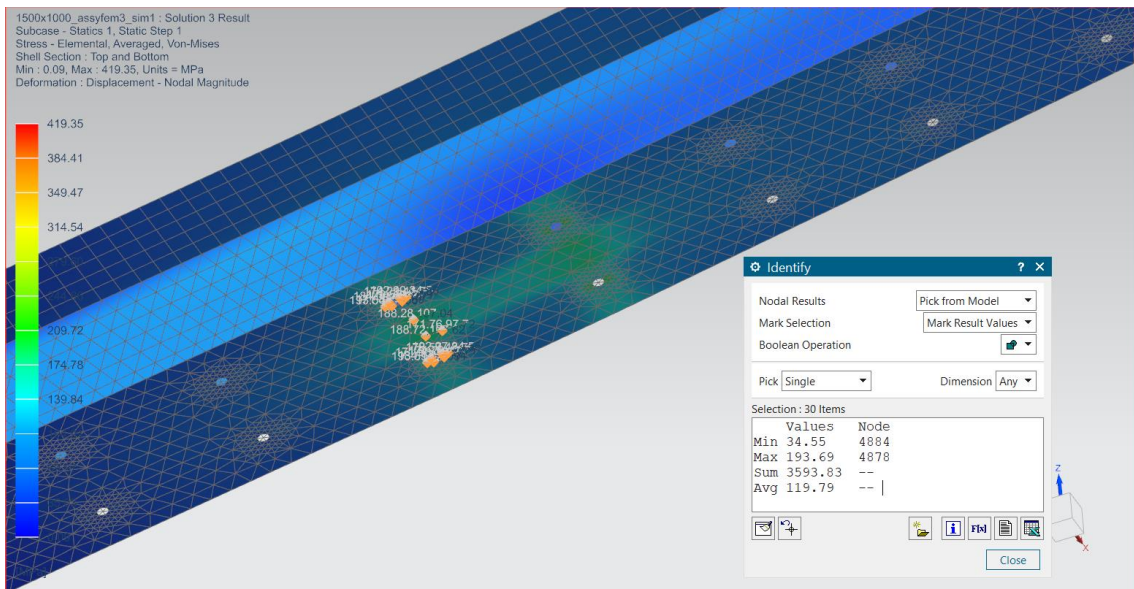
Image55. Von-mises next to the hole 10mm displacement.

As can be seen, the structure of the rotating bar begins to absorb part of the load, resulting in the stresses obtained in the area of application of the forces to grow. Using the identify results command and selecting the nodes next to the holes and those that support the most stress near this area, we obtain an average stress of 119.79 MPa and a maximum of 193.69 MPa.

- Configuration 3, 15 mm displacement.
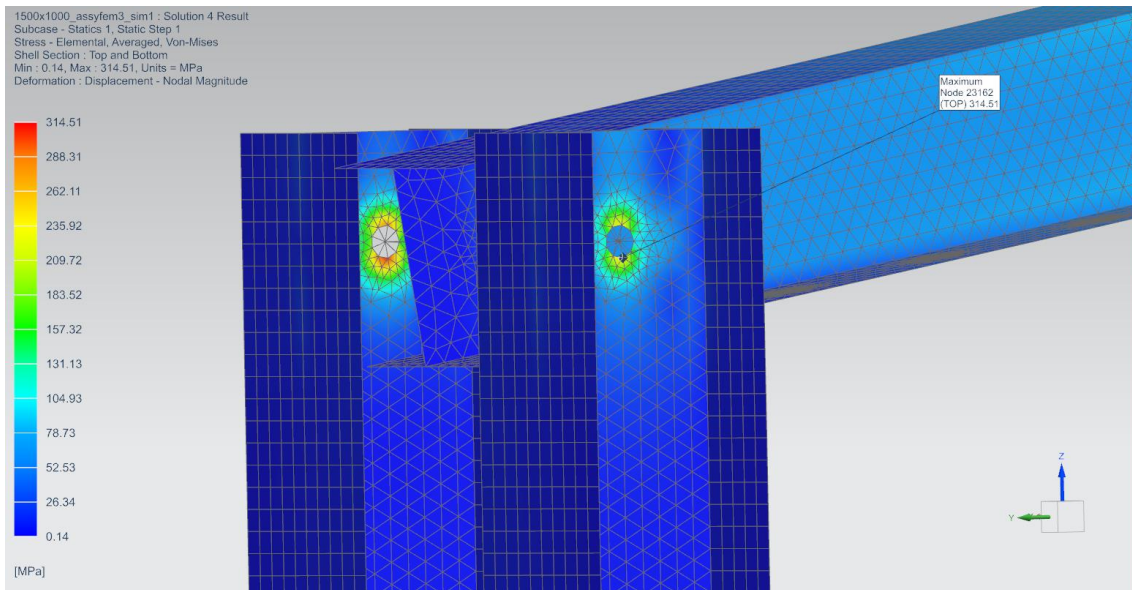
Image56. Von misses 15 mm displacement.

The maximum stress point is in the same place and also following the behavior observed when moving from one configuration to another in which the maximum Von-mises stress is reduced from one to another. The maximum Von-mises stress in this model is 314.51Mpa.
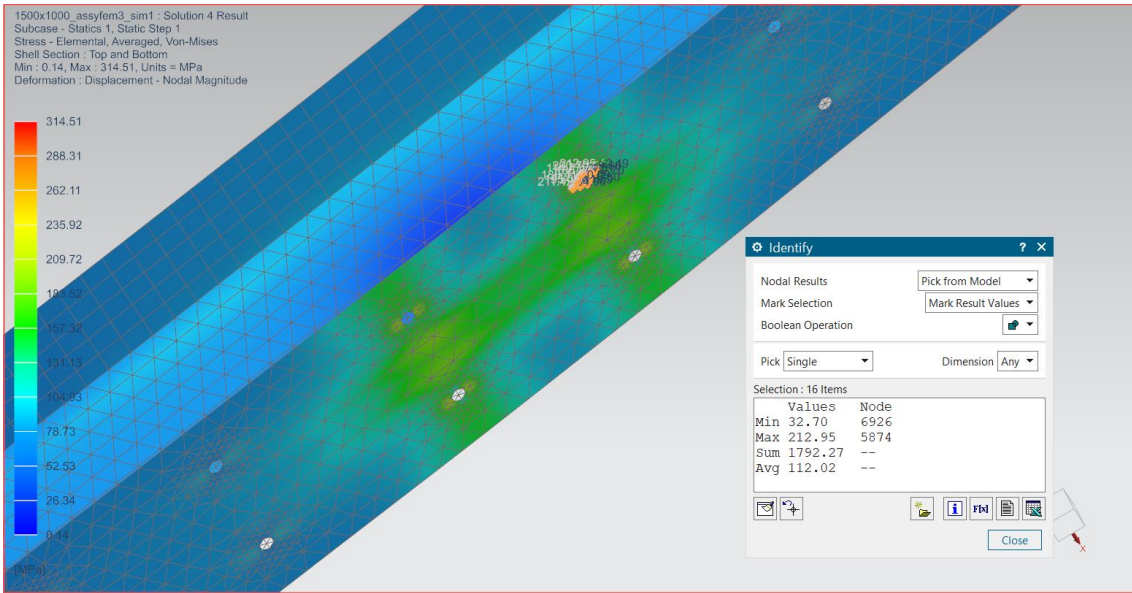
Image57. Von misses next to the hole 15 mm.

In this image it is observed how the value of the stress at the point of application of the forces

has grown, following the behavior observed between the different configurations. In this case

next to the hole the maximum stress is 212.95MPa and the average of 112.02 Mpa.
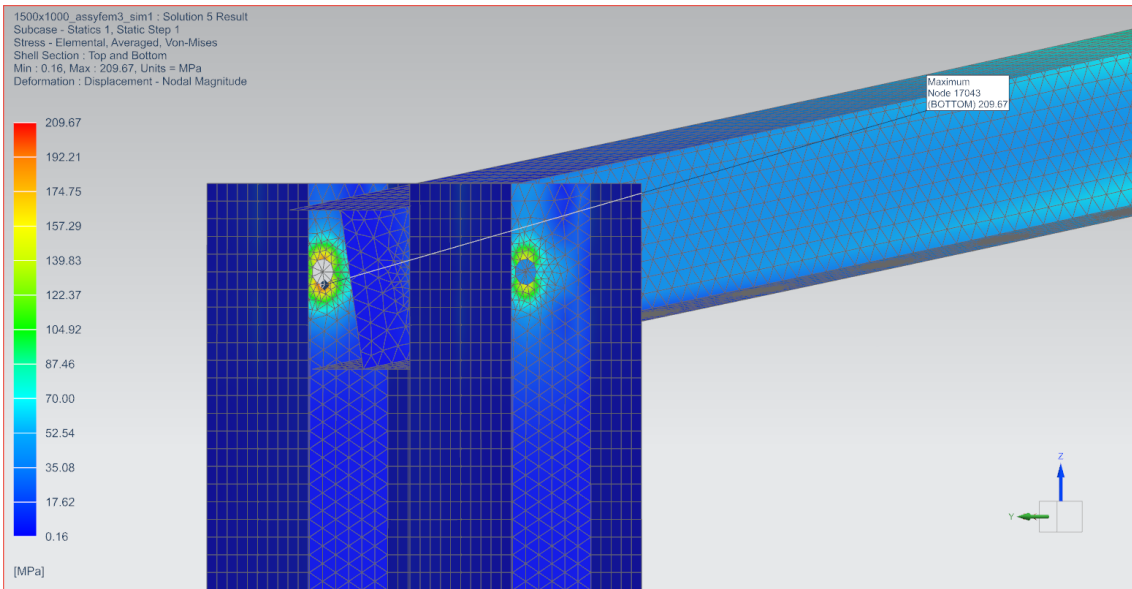
- Configuration 4, 20 mm displacement.

Image58. Von-mises 20mm displacement.

The maximum voltage of this point is 209.67 MPa, the lowest of all configurations but still in the same place as the previous ones.
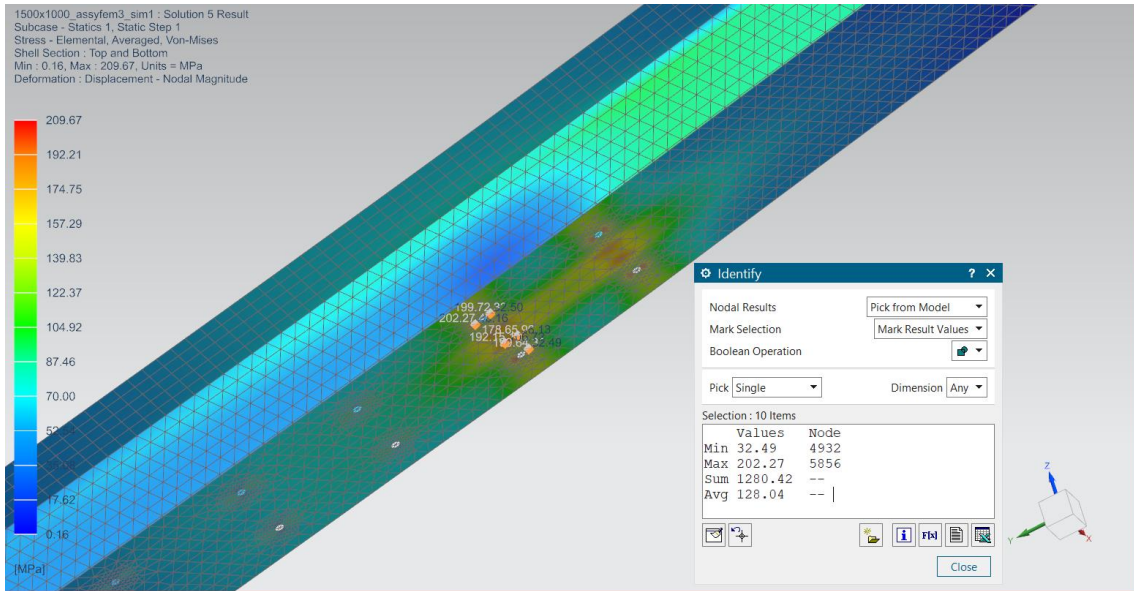
Image59. Von-mises next to the hole 20mm displacement.

In this photo we can see how clearly the stresses have been transferred to the rotating beam, the points of greatest stress are still the holes and the hitch area, but you can see how the color of the bar begins to change to colors between blue and green that indicate a stress around 70-120 MPa. The maximum voltage is in the lower zone and is about 202 MPa.

- Conclusions about the results.

		EN10025-2 Hot rolled products - Non-alloy structural steels			
Symbol	Description	S235	S275	S355	S450
f_y (MPa)	Yield strength	235	275	355	440
f_u (MPa)	Ultimate strength	360	430	490	550

Table5. Steel properties.

To begin with the interpretation of the results we will first start by looking at the point of the maximum Von-mises stress, located in the supporting beams. The value of this is 524.19 MPa, a value much higher than any of the Yield strengths of the steel that we have available in the table. Therefore, we can conclude that plastic deformation will occur during the test on the supporting beams, something that cannot happen and less during the performance of fatigue tests. It is true that at this point the deformation of the material is less than in the last point from which we obtained the 42 KN, we have applied this force in all the configurations of the system so that the reliability of the machine is greater and that there is a margin for the testing of materials that require a force greater than that of 42 KN. That said, it is necessary to use a material with mechanical characteristics superior to the steels of the table, the selected material is the Stainless Steel Grade15-5. This steel has a high yield strength, so will be a material that will better resist these stresses. In addition, the simulation of the system will be carried out again by changing the material of the support bars to check that now if the design conditions are met.

As for the rotating beam the point of maximum stress is in the last configuration, taking into account that this stress is 202.27 MPa, at no time is the yield strength exceeded. To obtain a higher safety coefficient and greater reliability of the machine, the steel used will be the S450 that has a yield strength of 440MPa.

$$\gamma = \frac{Yield\ strenght}{\sigma_{VM}} = \frac{440\ MPa}{202{,}27\ MPa} = 2{,}18$$

In this phase we will change the material of the support bars and perform the same tests with the same loads to study again the behavior of the bars and ensure that they do not break. The

material of the bar that rotates will not be modified since the behavior of this during the test is correct.

In this second simulation, the only points that will be studied are those that are part of the support beams, cause of not having changed the material of the bar that rotates its behavior will be the same during this simulation.
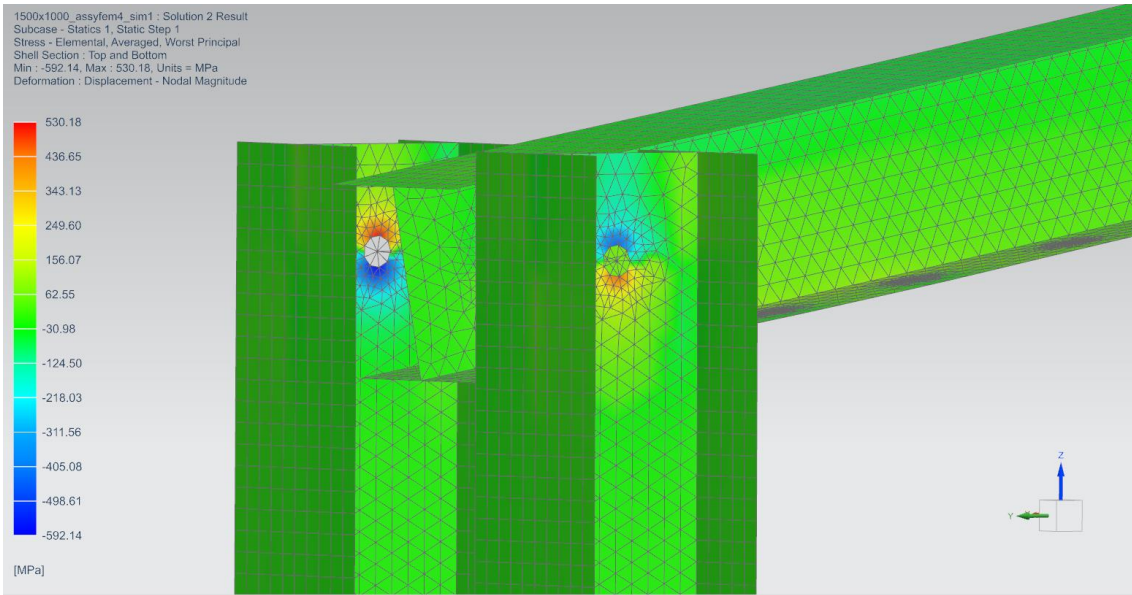
Change in the material to the Stainless Steel Grade15-5.
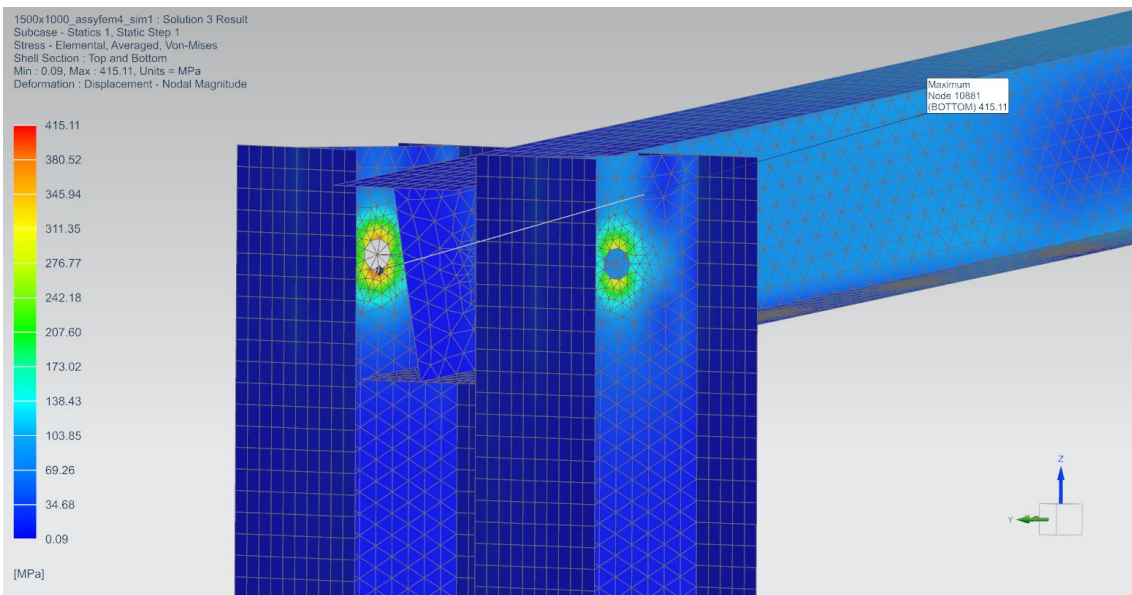
- Configuration 1, 5 mm displacement.
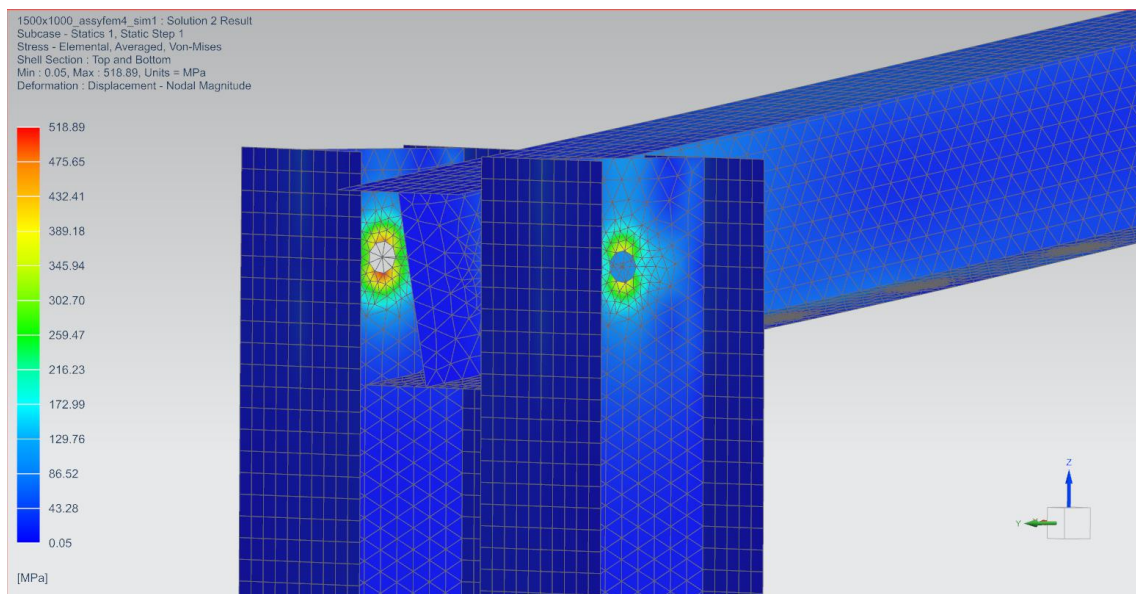
Image60. Von-mises Stainless Steel Grade15-5 5 mm displacement.

Image61. Worst principal inox 5 mm displacement.

- Configuration 2, 10 mm displacement.

Image62. Von-mises Stainless Steel Grade15-5 *10 mm displacement.*

- Configuration 3, 15 mm displacement.
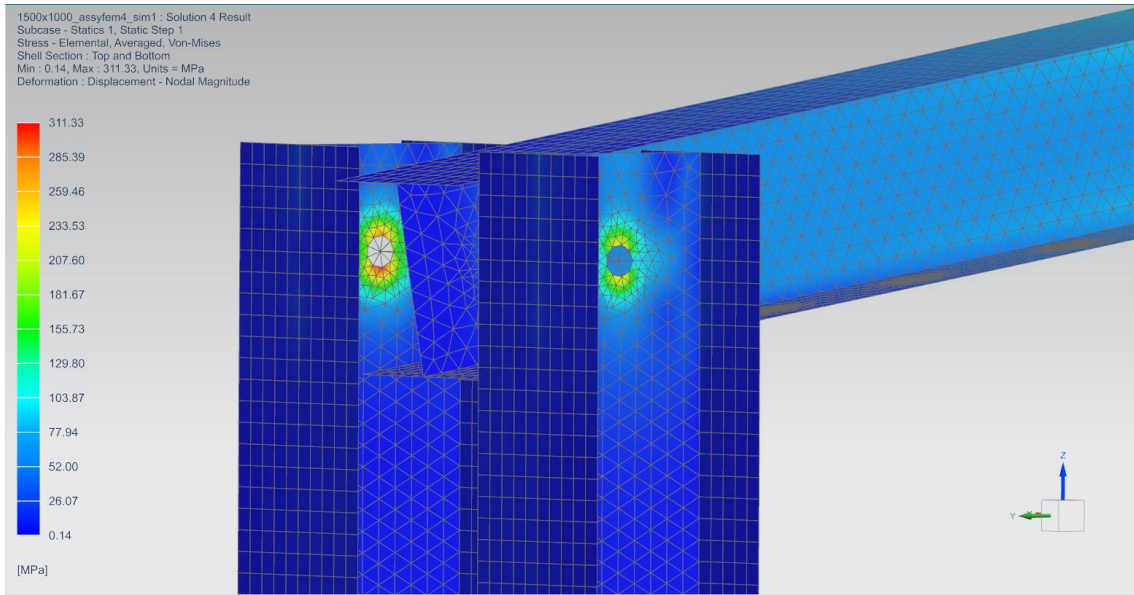
Image63. Von-mises Stainless Steel Grade15-5 *15 mm displacement.*

- Configuration 4, 20 mm displacement.
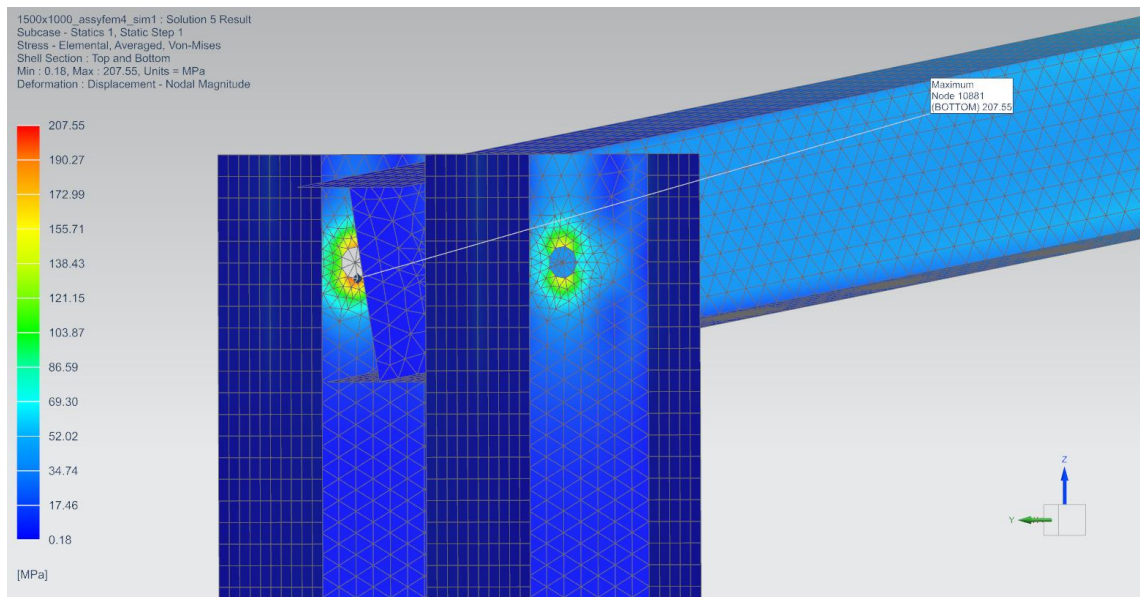
Image64. Von-mises Stainless Steel Grade15-5 *20 mm displacement.*

Obtaining the maximum Von-mises stress for each of the machine configurations is observed to follow the behavior of the previous simulation. The stress is reduced as the point of application of the forces moves away.

In this case the maximum Von-mises stress obtained throughout the machine is 518.89 MPa, this is in the first configuration as expected. Knowing the value of Stainless Steel Grade15-5 we obtain the following safety coefficient.

$$\gamma = \frac{Yield\ strenght}{\sigma_{VM}} = \frac{1275\ MPa}{518,89\ MPa} = 2,46$$

The use of this material ensures the reliability of the machine structure during the test and will be the material used for the construction of the same.

7.2.3.2 Modelling of the rest of the pieces of the machine.

The piece that connects the rotating bar with the gripping system and the steel tube.

For the modelling of this piece, the piece will be created in the same way that the bars were created and following the dimensions specified in the drawings, first the 3D figure is modeled and then the resulting 2D finally obtaining this result:
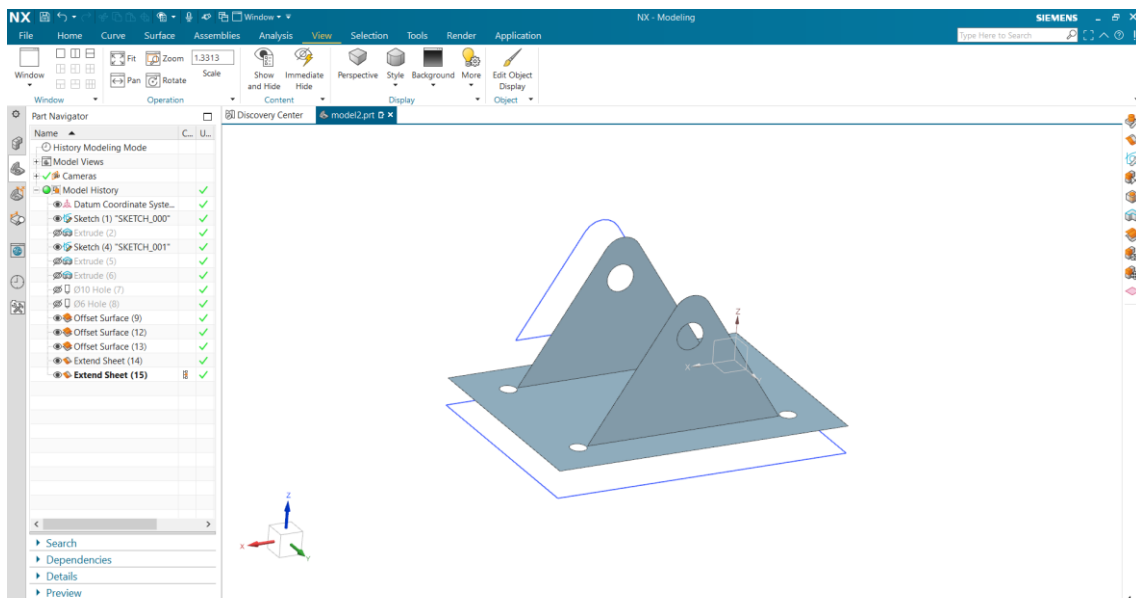

Image65. Piece 1 .prt model.

Following the previous steps on the Pre/post application create the physical properties of the

mesh. The material of this piece will be steel and the thickness of the walls will be also

introduced. For the introduction of the force on the point required, I will use RBE2 elements

and between this elements a tube that simulates the bolt where the force will be applied, with

this the most realistic results will be obtained and the mesh will look like this:
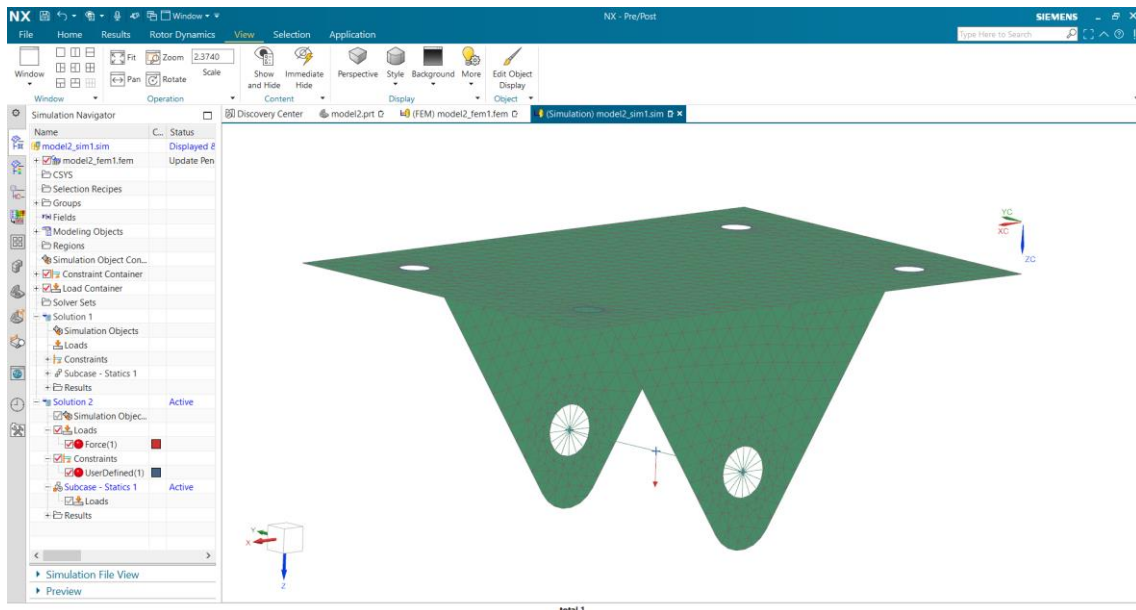
Image66. Piece 1 .sim model.

Once we have this we can move to the simulation, the constrains will be applied in the holes

simulating that the piece is attached to the rotating beam, and the force of 42KN will be

applied in the middle point of the bolt connexion.
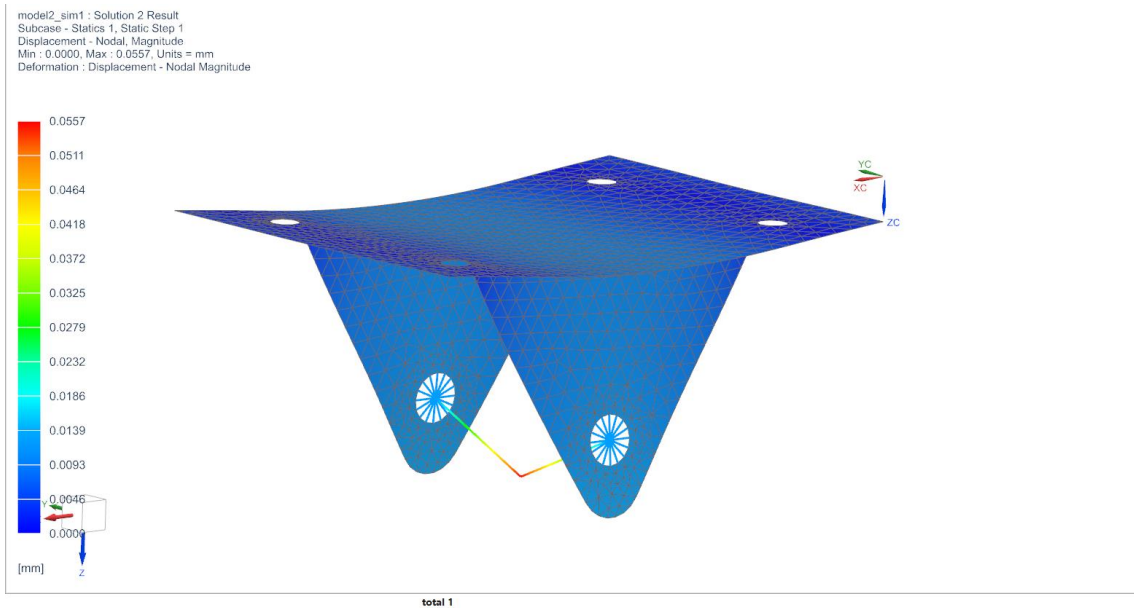
Image67. Deformation of the piece 1.
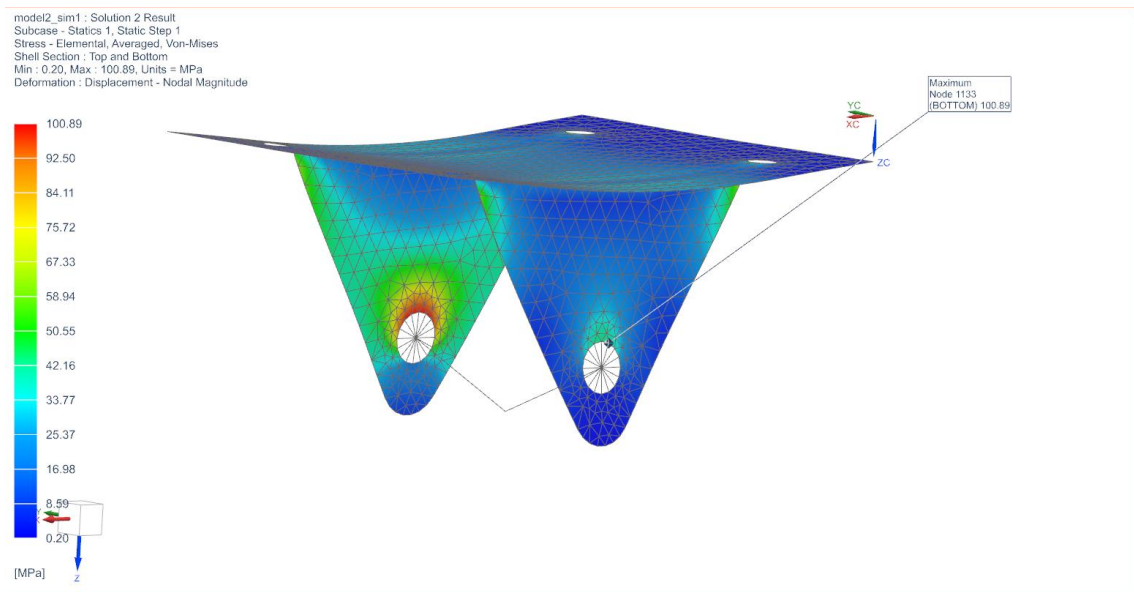
Image68. Von-mises of the piece 1.

In the same way as when analyzing the stresses concentrated in the structure of the beam, for the analysis of this piece the most critical points where the highest stresses are concentrated and the value of them will be observed. With this and comparing the value of these stresses with the yield strength again we can determine the behavior of the piece during the test. First, observing the displacement has a value of 0.0557 mm, this is an acceptable value also for the

point at which it is located. The maximum deformation is at the midpoint of the bolt where the force has been applied, that is why the bolts and connections used throughout the system cannot be of any material, they must be made of resistant materials and prepared to suffer some deformation without breaking. These will be more expensive but will ensure the stability of the system.

As for the stresses, the maximum stress you can see is in the proximity of the hole in the inner part of it, this makes sense due to the force to which the piece is subjected, other points that could also have been critical are the four holes that connect the piece with the beam, but as can be seen in this case they do not withstand great stress. The other critical points are in the union between the three bodies that make up the piece but is not the case. The maximum Von-mises stress is 100.89 MPa this does not compromise the resistance of the piece in any case and with this we can ensure a safety coefficient for the Steel 235.

$$\gamma = \frac{Yield\ strenght}{\sigma_{VM}} = \frac{235\ MPa}{100,89\ MPa} = 2,33$$

8. CONCLUSION.

As a conclusion for this project there are several points to be addressed. First of all, there are factors that during the realization of the design have been omitted in part due to the little influence on the design they had. One of these is regarding the displacement of the beam tracing a circular trajectory, this aspect influences the deformation of the specimens since this deformation will not occur only on one axis. This effect can produce a bending effect on specimens, but due to the low value of this displacement on the axis perpendicular to the desired one, at the point of greatest influence the value is less than 0.5mm. Even so, and to reduce the influence of this effect, several alternatives were tried. The first was that the

movement of the rotating bar was transferred to guides that only moved on the desired axis. But first of all, the difficulty in carrying it out and the difficulty in analyzing the behavior of the structure made us choose another option. This option is to install the parts that together with the gripping system allow rotation so that no unwanted stress accumulates in the specimen. In the case of requiring a modification due to this problem and for future projects, the modification mentioned before would be the most appropriate. It is also important to mention that during the design of the machine has always tried to simplify as much as possible to facilitate the use of it, in addition to taking into account the cost of production of the same was the lowest possible, for this and despite having to use relatively expensive materials for the support bars, all the mechanisms available to the machine have been designed trying to follow these two premises.

The mechanism that connects the motor to the rotating bar, the use of a spring that would transfer the movement to the bar was one of the possible options, the selected one is a simpler one in which it must be taken into account that the effort made by the bar and the pulley is relatively large so the material of this bar as much of the connections must be quite resistant, this is something that has not been able to be verified due to the lack of knowledge of how to add this type of structure to the model in which the resistance of the structure was simulated. Instead of that a displacement were added while doing the model in the desired axis. The machine has been tried to design following the standards imposed.

A point also to be discussed is the possibility of changing the configuration of the machine only by changing the length of the bar that joins the pulley with the rotating beam. In the current design the specimens are subjected to only traction, this could be done in the case of wanting to subject the specimens in a tensile-compression or only compression test. Finally, the initial knowledge regarding the simulation process with Nx has grown exponentially, the need to simulate structures outside of what was studied in class and the application of these to a real

design have made me realize the importance of this knowledge and have motivated me to

expand them in other programs and sectors. In addition to Nx, the following programs have

been used to carry out the project were Autocad, Excel and Word.

9. REFERENCES.

Connor, N. (2020, July 31). *What is high cycle fatigue vs low cycle fatigue - definition*. Material Properties. https://material-properties.org/what-is-high-cycle-fatigue-vs-low-cycle-fatigue-definition/

Introducción, 1. (n.d.). *Capítulo 2 Fatiga en materiales compuestos: comportamiento y mecanismos de degradación*. Tdx.Cat. Retrieved June 24, 2022, from https://www.tdx.cat/bitstream/handle/10803/6860/02CAPITULO.pdf?s

ISO 4965:1979. (2012). ISO. https://www.iso.org/standard/10984.html

Junkersfeld, K. (2018, November 11). *Ensayo de fatiga por resonancia: Principio de funcionamiento y aplicaciones comunes*. Linkedin.Com; LinkedIn. https://www.linkedin.com/pulse/ensayo-de-fatiga-por-resonancia-principio-y-comunes-klaus-junkersfeld?trk=related_artice_Ensayo%20de%20fatiga%20por%20resonancia%3A%20Principio%20de%20funcionamiento%20y%20aplaciones%20comunes_article-card_title

Macek, W., Zawiślak, S., Deptuła, A., & Ulewicz, R. (n.d.). Qpi-Journal.Pl. Retrieved June 24, 2022, from https://www.qpi-journal.pl/EN/files/2019_10_08.pdf

NX. (n.d.). Siemens Digital Industries Software. Retrieved June 24, 2022, from https://www.plm.automation.siemens.com/global/en/products/nx/

Table of material properties for structural steel S235, S275, S355, S420. (n.d.).

    EurocodeApplied.Com. Retrieved June 24, 2022, from

    https://eurocodeapplied.com/design/en1993/steel-design-properties

Weibull, W. (2013). *Fatigue testing and analysis of results*. Elsevier Science.

Wikipedia contributors. (2022, June 7). *Fatigue testing*. Wikipedia, The Free
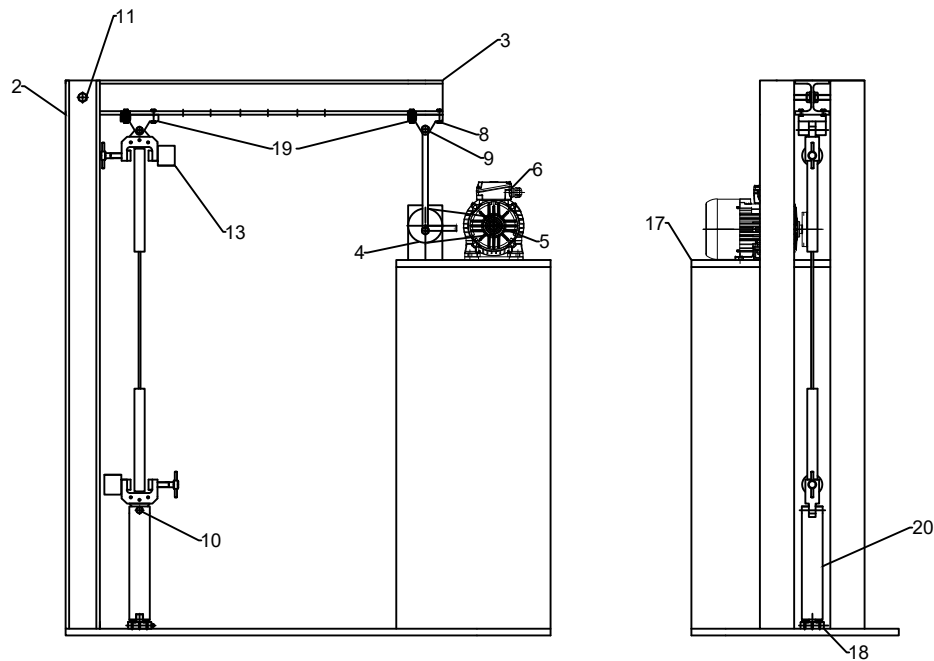
    Encyclopedia.

    https://en.wikipedia.org/w/index.php?title=Fatigue_testing&oldid=109

    1926586

(N.d.). Upv.Es. Retrieved June 24, 2022, from

    https://www.upv.es/materiales/Fcm/Fcm02/fcm2_4.html

10. PREPARATION OF THE TECHNICAL DOCUMENTATION.
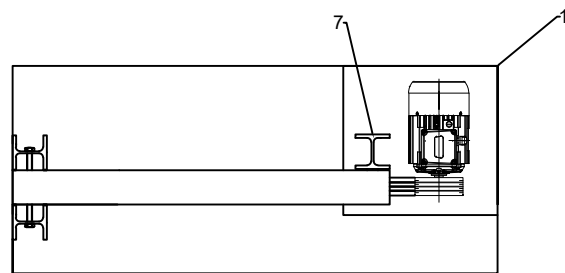
ITEM Nº	ELEMENT NAME	QUANTITY	STANDARD Nº	MATERIAL
20	Steel tube	1		S235JR
19	Connection piece	2		S235JR
18	Force sensor	1		
17	Motor supporting structure	1		S235JR
16	Washer M15	2		
15	Nut M12	4		
14	Nut M6	8		
13	Gripping system	1		
12	Nut M15	3		
11	Bolt M15x215	1	ISO 1665	
10	Bolt M12x60	1	ISO 1665	
9	Bolt M12x80	3	ISO 1665	
8	Bolt M6x30	8	ISO 1665	
7	Driven pulley supporting structure	1		S235JR
6	Motor	1		
5	Driver pulley	1		
4	Driven pulley	1		
3	Rotating beam	1		S450
2	Supporting beam	2		S/Steel_PH15-5
1	Suporting structure	1		S235JR

University Name	Name of Element
PWR	Machine assembly

Designer	Approve Staff
Pablo López	Grzegorz Lesiuk

Scale	Form	No. of Drawing	Date
1:10	A2	00	23.06.2022

M15

50

50

1600

100

R12

100

110

1100

100

100

M15

M6

50

50

176,67

80

86,67

80

10

25

University Name		Name of Element
PWR		Gripping system.
Designer		Approve Staff
Pablo López		Grzegorz Lesiuk

Scale	Form	No. of Drawing	Date
1:1	A2	13	23.06.2022

M20

Ø8,4

42

19

8

68

76

50

University Name		Name of Element	
PWR		Force sensor.	
Designer		Approve Staff	
Pablo López		Grzegorz Lesiuk	
Scale 1:1	Form A3	No. of Drawing 18	Date 23.06.2022
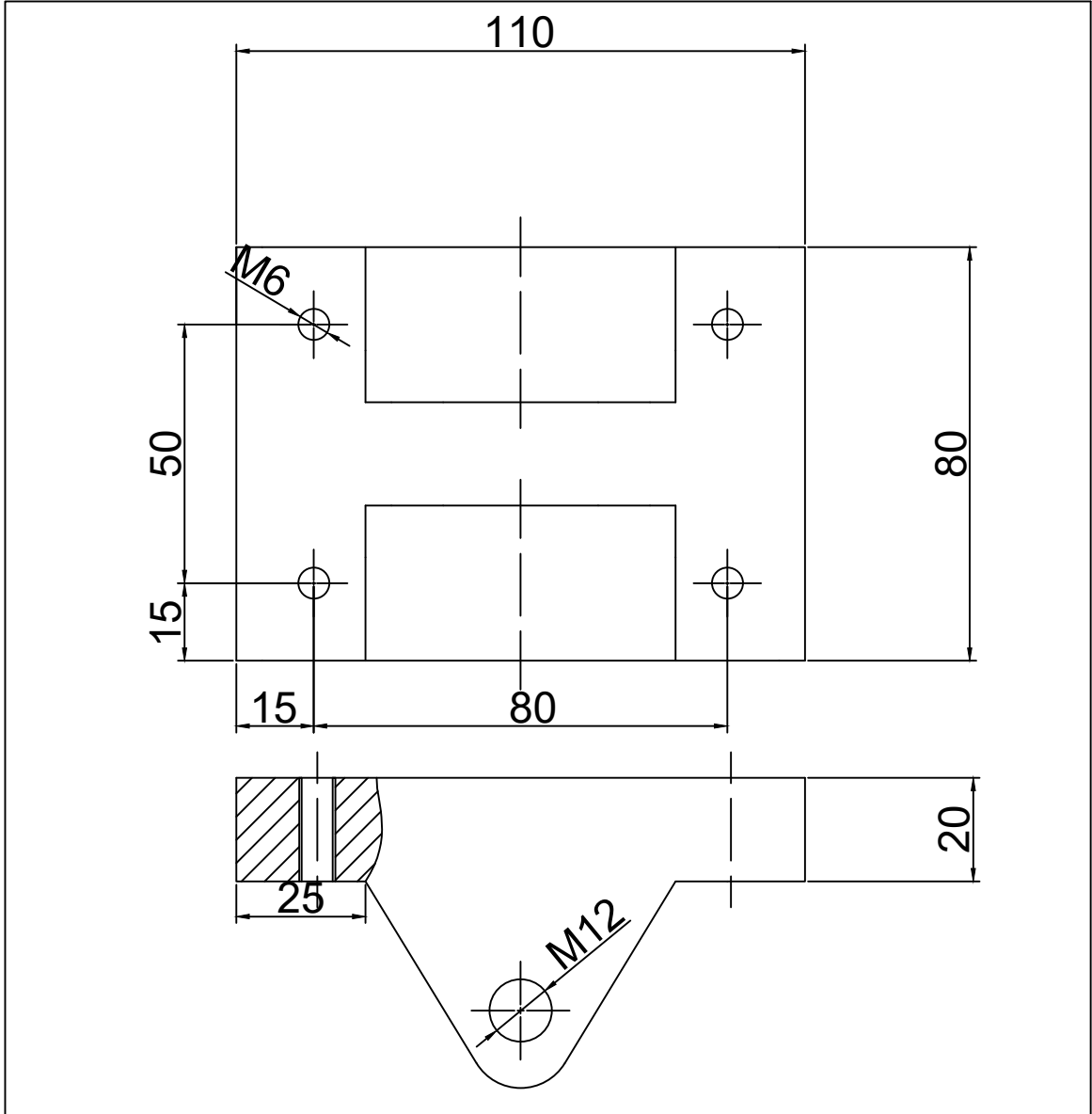
University Name		Name of Element	
PWR		Connection piece.	
Designer		Approve Staff	
Pablo López		Grzegorz Lesiuk	
Scale	Form	No. of Drawing	Date
1:1	A3	19	23.06.2022

M12

20 20 20

35

330

M20

Ø60

University Name		Name of Element	
PWR		Steel tube.	
Designer		Approve Staff	
Pablo López		Grzegorz Lesiuk	
Scale	Form	No. of Drawing	Date
1:1	A2	20	23.06.2022